

**SECTION D**

**Responses to NRC Questions on WCAP-8859 (Non-Proprietary)  
and WCAP-8860 (Non-Proprietary)**



Westinghouse Electric Corporation

Power Systems

Box 355  
Pittsburgh Pennsylvania 15230

NS-CE-1694

February 13, 1978

Mr. John F. Stolz, Chief  
Light Water Reactors Branch  
Division of Projects Management  
Office of Nuclear Reactor Regulation  
U.S. Nuclear Regulatory Commission  
Washington, D.C. 20555

- References:
- (1) Letter from C. Eicheldinger to J. F. Stolz, NS-CE-1219, dated September 29, 1976.  
Subject: TRANFLO Steam Generator Code Description, WCAP-8821(P) and WCAP-8859 (Non-Proprietary)
  - (2) Letter from C. Eicheldinger to J. F. Stolz, NS-CE-1220, dated September 29, 1976.  
Subject: Mass and Energy Releases Following a Steam Line Rupture, WCAP-8822(P) and WCAP-8860 (Non-Proprietary)
  - (3) Letter from J. F. Stolz to C. Eicheldinger, dated April 19, 1977.  
Subject: Request for additional information on WCAP-8822(P), WCAP-8859 (Non-Proprietary) and WCAP-8860 (Non-Proprietary)

Dear Mr. Stolz:

Enclosed are:

1. Forty (40) copies of additional information on WCAP-8821 (Proprietary) and WCAP-8822 (Proprietary),
2. Twenty (20) copies of additional information on WCAP-8859 (Non-Proprietary) and WCAP-8860 (Non-Proprietary),

as requested by Reference 3.

Also enclosed are one (1) copy of Application for Withholding, AW-76-45 (Non-Proprietary), and one (1) copy of Affidavit (Non-Proprietary).

John F. Stolz  
February 13, 1978  
Page Two

This submittal contains proprietary information. In conformance with the requirements of 10CFR Section 2.790, as amended, of the Commission's regulations, we are endorsing with this submittal an application for withholding from public disclosure and an affidavit. The affidavit identifies the information sought to be withheld and sets forth the basis on which the information may be withheld from public disclosure by the Commission.

We expect that the non-proprietary version of this information will be placed in the Public Document Room and identified as supporting information to the WCAP's identified above.

Correspondence with respect to the Westinghouse affidavit or application for withholding should reference AW-78-13 and should be addressed to: R. A. Wiesemann, Manager, Licensing Programs, Westinghouse Electric Corporation, P.O. Box 355, Pittsburgh, Pennsylvania 15230.

Very truly yours,

WESTINGHOUSE ELECTRIC CORPORATION



C. Eicheldinger, Manager  
Nuclear Safety Department

REL/mj  
Enclosures

### QUESTION 1.1

An approximation for the conservation of momentum equation is given in equations 3 through 8. Provide a detailed derivation of this equation. Discuss and justify all assumptions. Compare this method to that used in the SATAN-VI code.

Answer 1.1

The basic one-dimensional momentum equation is -

$$\frac{\partial(W/A)}{\partial t} + \frac{\partial}{\partial z} (WV) = - \frac{\partial P}{\partial z} - F \frac{vW|W|}{2D_h A^2} - \bar{\rho}g \quad (1)$$

where

- W = mass flow
- V = fluid velocity
- P = pressure
- D<sub>h</sub> = hydraulic diameter
- $\bar{\rho}$  = average density
- v = specific volume
- F = friction factor
- A = channel flow area

Integrating (1) along the length of a flow path gives -

$$\int_1^2 \frac{\partial(W/A)}{\partial t} dz = (P_2 - P_1) - \int_1^2 \frac{\partial(WV)}{\partial z} dz - \int_1^2 \frac{FvW|W|}{2D_h A^2} dz - \int_1^2 \bar{\rho}g dz \quad (2)$$

This can be written as

$$\int_1^2 \frac{\dot{W}}{A} dz = (P_2 - P_1) - \int_1^2 \frac{\partial(WV)}{\partial z} dz - \int_1^2 \frac{FvW|W|}{2D_h A^2} dz - \int_1^2 \bar{\rho}g dz \quad (3)$$

If the flowrate, W, is assumed uniform in the channel

$$\int_1^2 \frac{\dot{W}}{A} dz = \frac{L_{12}}{A} \dot{W} \quad (4)$$

Also, if the frictional losses are functions only of  $W$ , and  $W$  is uniform -

$$\int_1^2 \frac{F_W |W|}{2D_h A^2} dz = \frac{1}{2\rho} \left( \frac{FL'}{D_h} \right)_{12} \frac{W|W|}{A^2} \quad (5)$$

And

$$\int_1^2 \bar{\rho} g dz = \bar{\rho} g (Z_2 - Z_1) \quad (6)$$

where  $L_k$  = initial length of the flow channel  
 $\dot{W}$  = time derivative of the flow rate  
 $Z$  = elevation  
 $L'$  = equivalent frictional length for the flow channel

Thus

$$\frac{L_{12}}{A} \dot{W} = (P_2 - P_1) - \int_1^2 \frac{\partial(WV)}{\partial z} dz - \frac{1}{2\rho} \left( \frac{FL'}{D_h} \right) \frac{W|W|}{A^2} - \bar{\rho} g (Z_2 - Z_1) \quad (7)$$

Now consider the acceleration force term  $\partial(WV)$ .

For a two phase fluid with different phase velocities -

$$\int_1^2 \frac{d(WV)}{dz} dz = \int_1^2 \left[ \frac{d(W_E V_E) + d(W_F V_F)}{A} \right] \quad (8)$$

where  $V_g$  and  $V_F$  are the phase velocities. However -

$$V_g = \chi W / \alpha A \rho_g \quad (9)$$

$$V_F = (1-\chi) W / (1-\alpha) A \rho_F \quad (10)$$

$\alpha$  = void fraction

$\chi$  = flow quality

Letting  $X = \left[ \frac{(1-\chi)^2}{(1-\alpha)} + \frac{\chi^2}{\alpha} \frac{\rho_F}{\rho_g} \right] \frac{1}{\rho_F}$  equation (8) becomes (11)

$$\Delta P \text{ acceleration} = W^2 \int_1^2 \frac{1}{A} d \left( \frac{X}{A} \right) \quad (12)$$

If both the density and flow area are variable over the length of the channel equation (12) can be approximated by

$$\Delta P \text{ acceleration} = \frac{W^2}{2} \left[ \frac{1}{A_2} + \frac{1}{A_1} \right] \left[ \frac{X_2}{A_2} - \frac{X_1}{A_1} \right] \quad (13)$$

as is shown in Reference 10.

Substituting this result into equation (7)

$$\frac{L_{12}}{A} \dot{W} = (P_2 - P_1) - \frac{1}{2\rho} \left( \frac{FL'}{D_h} \right) \frac{W|W|}{A^2} - \bar{\rho}g(Z_2 - Z_1) - \frac{W^2}{2} \left[ \frac{1}{A_2} + \frac{1}{A_1} \right] \left[ \frac{X_2}{A_2} - \frac{X_1}{A_1} \right] \quad (14)$$

Letting  $\frac{L_{12}}{A} = L_k$

$$\bar{\rho} = 1/2 (\rho_1 + \rho_2) \quad (15)$$

and 
$$\frac{FL}{D_h} = \frac{FL_{12}}{D_h} + FD \quad (16)$$

then-

$$L_k \dot{W} = (P_2 - P_1) - \frac{1}{2\rho} \frac{FL_{12}}{D_h} \frac{W|W|}{A^2} - g \left( \frac{\rho_1 + \rho_2}{2} \right) (z_2 - z_1) - \frac{W^2}{2} \left[ \frac{1}{A_2} + \frac{1}{A_1} \right] \left[ \frac{X_2}{A_2} - \frac{X_1}{A_1} \right] - \frac{1}{2\rho} \frac{FD}{A^2} \frac{W|W|}{A^2} \quad (17)$$

where  $FD = \text{equivalent } \frac{FL}{D}$  for non-recoverable pressure losses in the channel due to obstructions, area changes, etc.

Approximating  $F$  by the Blasius equation [Reference 9]  $F = 0.316 \text{ Re}^{-1/4}$  gives (18)

$$\dot{W} = \frac{1}{L_K} [P_2 - P_1] - (0.316 \text{ Re}^{-1/4}) \frac{L_{12} W|W|}{2D_h A^2} - \left( \frac{FD v}{2 A^2} \right) - \frac{g}{2} \left( \frac{1}{v_1} + \frac{1}{v_2} \right) (z_2 - z_1) \left( \frac{1}{A_2} + \frac{1}{A_1} \right) \left( \frac{X_2}{A_2} - \frac{X_1}{A_1} \right) \frac{W^2}{2} \quad (19)$$

Equation (19) with appropriate conversion constants introduced for dimensional consistency is identical to equation (3) on page 3-1 of WCAP-8821. This equation is essentially the same equation that has been used effectively by Nahavandi (1)(10), Margolis (11), Meyer and many others to predict transient flow situations in two-phase steam/water systems.

Chief differences between the above equation and that used in SATAN are listed below (8):



- 1) SATAN defines  $F = 0.0055 \left[ 1 + \left( 20000 \frac{E}{D} + \frac{10^6}{R_e} \right)^{1/3} \right]$  for single phase friction Factors.
- 2) SATAN uses the HTFS correlation for two-phase friction multipliers which are then used to modify the single phase frictional loss to account for the higher pressure drops in two-phase situations.
- 3) The acceleration pressure drop due to density and area changes are developed in an entirely different manner in SATAN as can be seen by reviewing pages 2-26 through 2-29 of Reference 9.
- 4) SATAN also includes pressure drop due to mixing, compressibility, and pump elements which are not included in the TRANFLØ equation.

## QUESTION 1.2

Page 2-12 of WCAP-8822 states that the heat transfer correlations used in the TRANFLO code to calculate primary-to-secondary heat transfer are designed to underpredict heat flow and thereby minimize entrainment.

- A. For each correlation listed in Section 3.4 of WCAP-8821, provide justification that heat transfer to the steam generator is conservative for calculation of entrainment.
- B. Provide additional details on the use of each correlation for heat transfer between (1) the primary system and the steam generator tubes and (2) the steam generator tubes and the secondary secondary for both the broken and intact loop steam generators. Provide the criteria for switching between correlations used in the TRANFLO code.
- C. Discuss the form of the Westinghouse transition boiling correlation used in the TRANFLO code. We understand that the correlation exists in a best estimate form and also in a form for ECCS LOCA calculations.

## Answer 1.2

Page 2-12 of WCAP-8822 does not state that the heat transfer correlations used in TRANFLO are designed to underpredict heat flow. Instead, the statement is made that the primary temperature transients (input to TRANFLO) were selected such that energy transfer to the secondary side of the steam generator is conservatively low. Minimizing the energy transfer to the secondary side during a blowdown results in a lower steam pressure, and therefore, a lower blowdown flowrate. The lower flowrate, in turn, results in a higher average quality of the blowdown effluent.

The heat transfer relationships described in Section 3.4 of WCAP-8821 were chosen because they are commonly used, accepted, and appropriate empirical correlations to predict heat transfer in steam, steam/water, and compressed water systems. They are not selected to either overpredict or underpredict heat transfer, but were selected instead to predict accurately the actual energy transfer for a given set of thermodynamic conditions. Selection of the appropriate correlation from among those described in WCAP-8821 is accomplished using the logic illustrated on the attached flow chart. Also shown on the flow chart is the manner in which the primary film, tube, and secondary film coefficients are combined to give an overall heat transfer coefficient from the primary to the secondary.

The calculational methods discussed above and on the attached chart were used only for the steam generator with the broken steam line. Even then, the calculation was used only as part of the TRANFLO calculation of moisture entrainment versus time which was later used as input data to the MARVEL code. The MARVEL code, using the input entrainment information, then determined the heat transfer to both the steam generators with intact lines and the steam generator blowing down. The techniques of determining steam generator heat transfer in MARVEL are discussed in WCAP-8843, section 2.17.

Finally, the MARVEL calculated heat transfer to the faulted steam generator was checked to ensure conservatism with respect to the TRANFLO

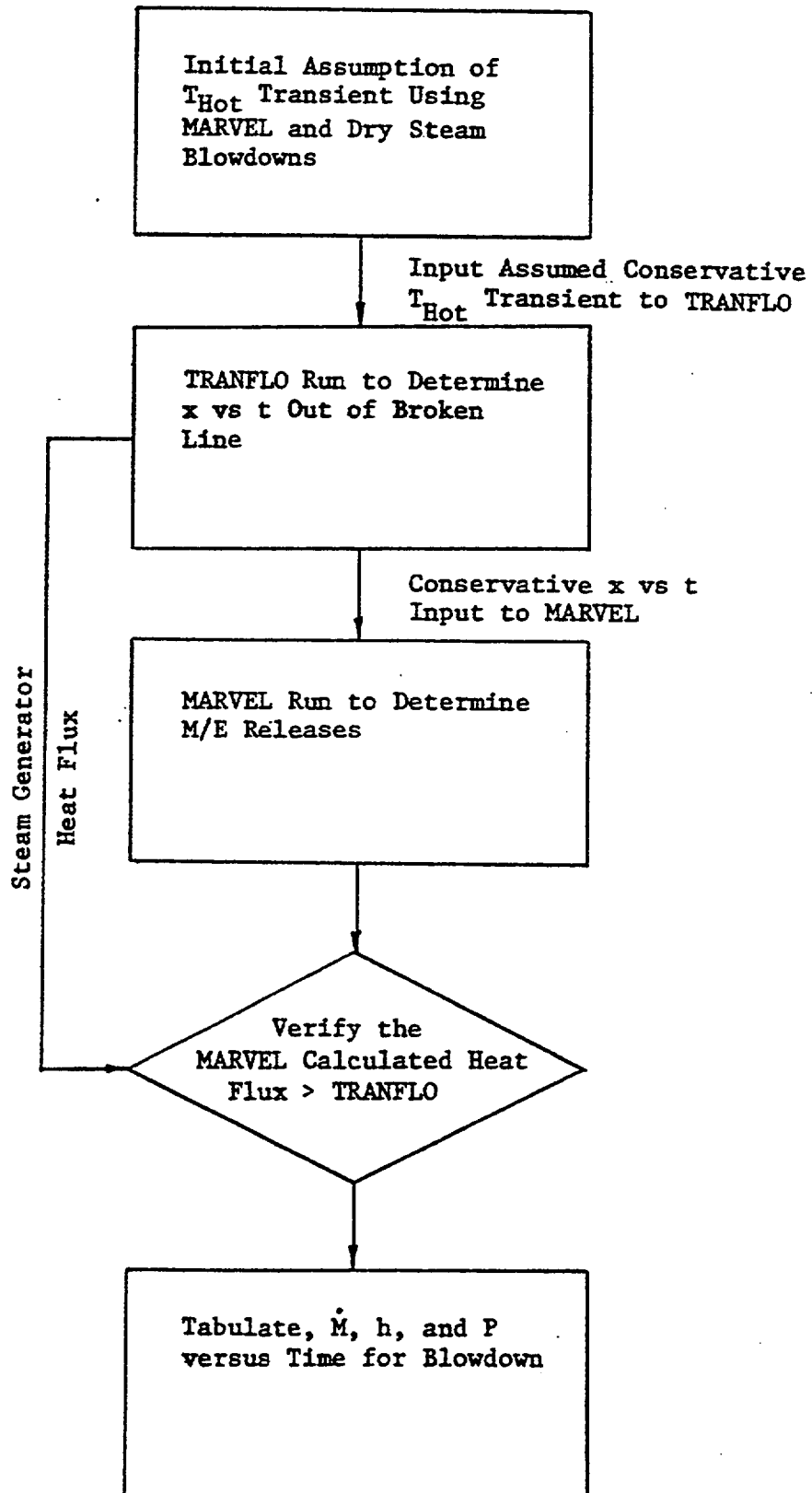
calculations (see Section 3.2.1 of WCAP-8822). For clarification, a logic block diagram of the analysis steps used for determining the releases from the various breaks is attached.

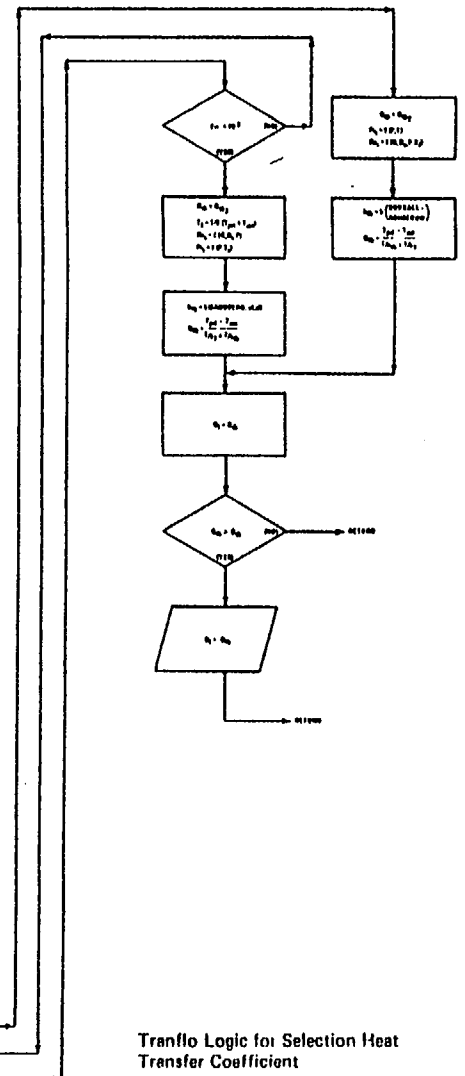
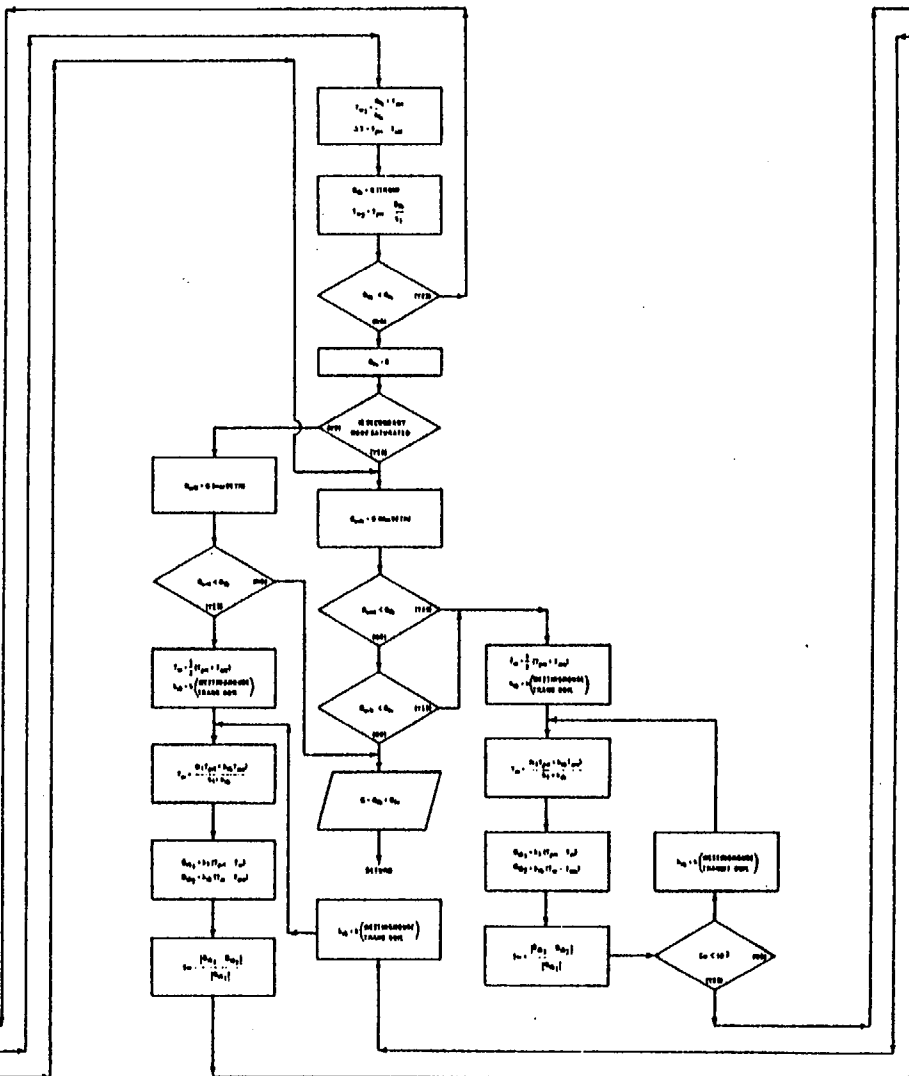
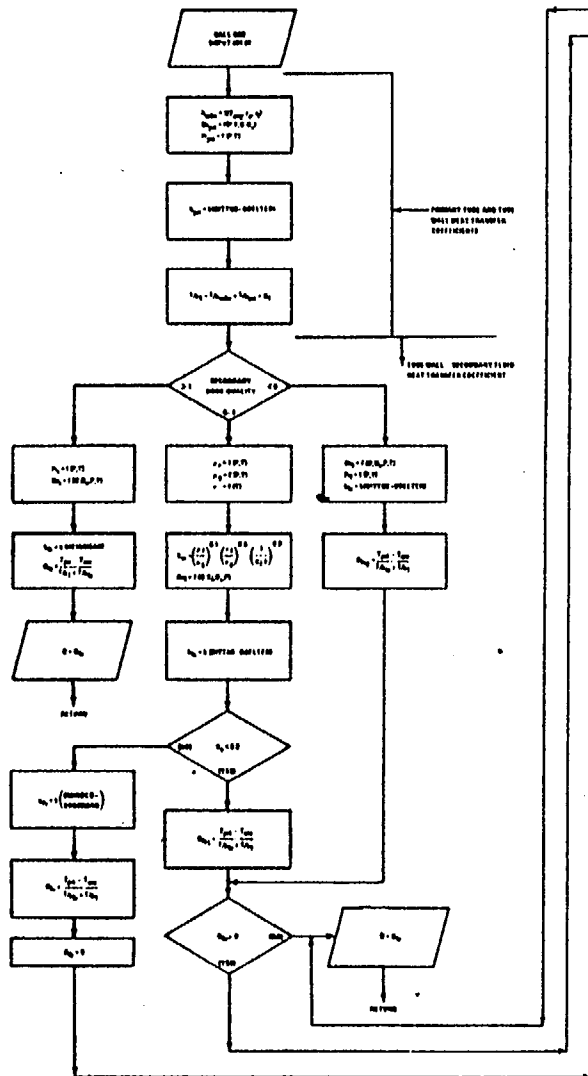
Westinghouse Transition Boiling Correlation

Although included in the TRANFLO heat transfer logic, transition boiling is not a factor during steam line break transients. In none of the blow-downs presented in WCAP-8822 do the calculations indicate operation in this regime. Therefore, the form of the equation used is not believed to be important. Nevertheless, the form used in TRANFLO is similar to the ECCS-LOCA correlation, i.e.

(a,c)

SEQUENCE OF DATA TRANSFER FROM TRANFLO TO MARVEL





Tranflo Logic for Selection Heat Transfer Coefficient

### QUESTION 1.3

Discuss how the values of primary system temperature, flow rate and pressure at the steam generator inlet are determined from the MARVEL code so as to be conservative for use in the entrainment calculations of the TRANFLO code. Discuss how primary system properties within the steam generator tubes are determined for use in the TRANFLO nodal heat transfer calculations.

### Answer 1.3

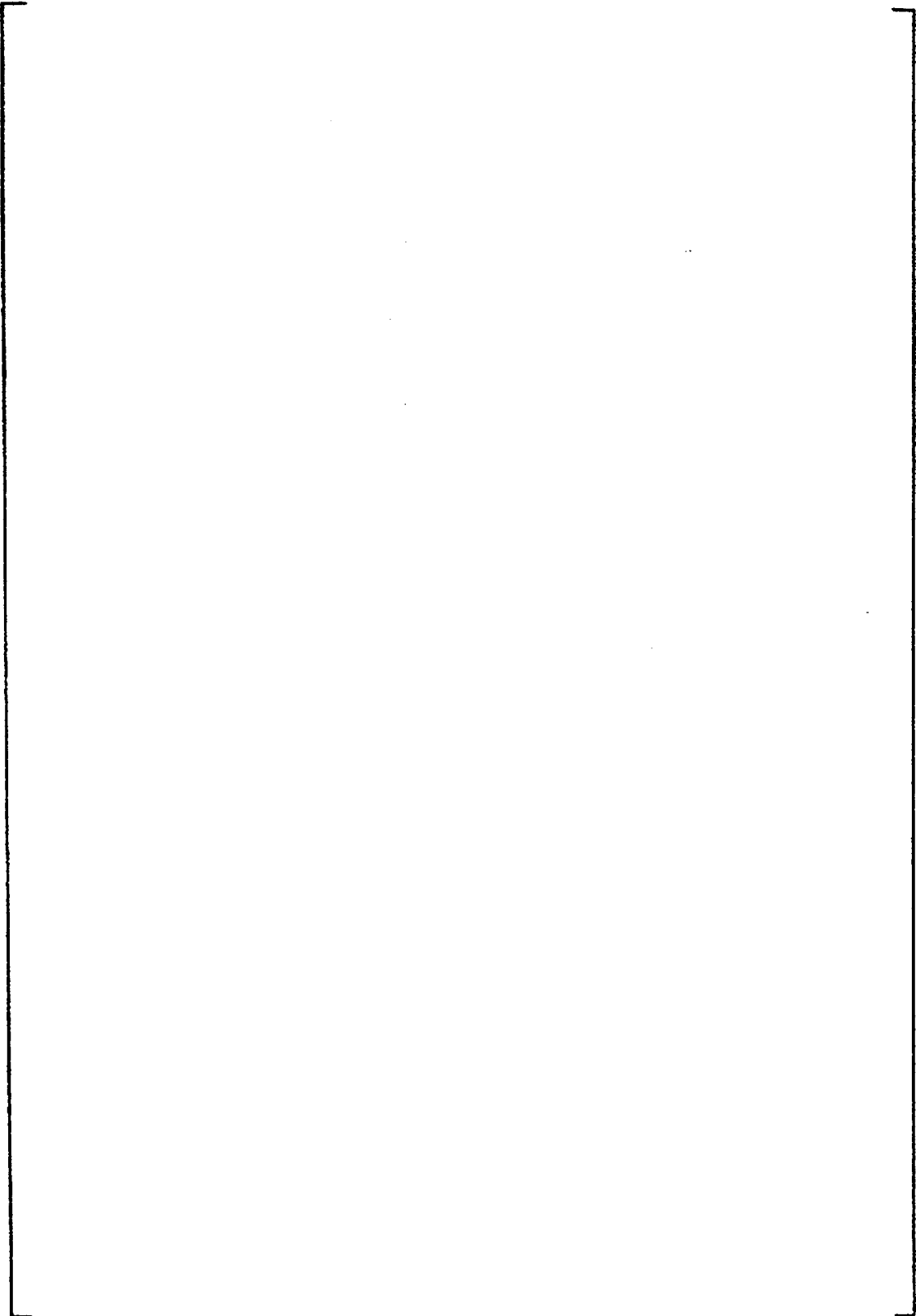
The input data to TRANFLO specifying the primary system conditions for blowdown calculations assumed a constant primary flow equal to nominal loop flow and a constant primary system pressure of 2250 psia. Two different hot leg temperature histories were used depending upon the break size. For all the intermediate and small breaks analyzed, a constant temperature profile was used. For the full double-ended ruptures a decaying temperature history was selected based upon initial MARVEL studies in which dry steam blowdowns were assumed. The temperature history was chosen so that it represented the downward trend of the primary hot leg temperature but was always above the MARVEL predicted temperature. The attached figure compares the TRANFLO input temperatures with the calculated MARVEL results for representative cases.

The primary system properties through the steam generator tubes are determined in TRANFLO from the inlet conditions described above and an energy balance on each heat transfer segment. The energy balance determines the primary fluid temperature for each successive tube segment based on the energy removed in the preceding segments. The primary fluid is assumed to be compressed liquid at all times; thus, the flow rate and pressure are held constant throughout the tube bundle. Fluid properties are determined for each heat transfer segment based on the temperature calculated for that segment.



PRIMARY TEMPERATURE TRANSIENT FOR STEAMBREAK  
BLOWDOWN CALCULATION

(a,c)



QUESTION 1.4

Provide a derivation of the equation on page 3-9 for two-phase quality in the flow paths starting with the work of Armand discussed in reference 5 to WCAP-8821.

Answer 1.4

The equation for  $\chi_f$  on Page 3-9 has a typographical error. The term shown as the denominator should instead be added to the term shown as the numerator. The resulting equation, when this change is made, was derived from Armand's original work by W. A. Massena (see References 1 and 2), and includes a correction by Massena to eliminate a discontinuity in the original work which occurred at  $\chi_\alpha=0.75$ . This equation is generally called the "modified Armand correlation" and has the form:

$$\alpha = \frac{(0.833 + 0.167\chi)\chi\beta}{(1-\chi) + \beta\chi}$$

where

$\alpha$  = void fraction ( $\chi_\alpha$ )

$\chi$  = quality ( $\chi_f$ )

$\beta$  = slip ( $v_s/v_w$ )

This can be re-arranged as follows to arrive at the subject equation:

$$\chi^2 + \chi \{[\alpha + (0.833 - \alpha)\beta] / 0.167\beta\} - (\alpha / 0.167\beta) = 0$$

$$\chi^2 + \chi \{[\alpha + (\frac{5}{6} - \alpha)\beta] / \frac{\beta}{6}\} - (6\alpha/\beta) = 0$$

$$\chi^2 + \chi \{[\alpha(1-\beta) + \frac{5}{6}\beta] / \frac{\beta}{6}\} - (6\alpha/\beta) = 0$$

$$\chi^2 + \chi \{[6\alpha(1-\beta) + 5\beta] / \beta - (6\alpha/\beta)\} = 0$$

$$\chi = -2.5 - 3\alpha \left(\frac{1}{\beta} - 1\right) \pm \frac{1}{2} \left\{ \left(6\alpha \left(\frac{1}{\beta} - 1\right) + 5\right)^2 + \frac{24\alpha}{\beta} \right\}^{1/2}$$

$$= -2.5 + 3\alpha \left(1 - \frac{1}{\beta}\right) \pm \left\{ \left(2.5 - 3\alpha \left(1 - \frac{1}{\beta}\right)\right)^2 + 6\alpha \left(\frac{1}{\beta}\right) \right\}^{1/2}$$

Using  $\beta = v_s/v_w$ ,  $\chi = \chi_f$  and  $\alpha = \chi_\alpha$

$$\chi_f = -2.5 + 3\chi_\alpha \left(1 - \frac{v_w}{v_s}\right) \pm \left\{ \left[2.5 - 3\chi_\alpha \left(1 - \frac{v_w}{v_s}\right)\right]^2 + 6\chi_\alpha \left(\frac{v_w}{v_s}\right) \right\}^{1/2}$$

The requirement that  $\chi_f = 0$  when  $\chi_\alpha = 0$  requires that the negative sign on the square root term then be dropped.

QUESTION 1.5

The reference for the two-phase multiplier correlation by Murdock appears to be in error. Please provide this reference. Discuss the applicability of this correlation for calculation of friction pressure drops as used in equation 5 and for form loss pressure drops as in equation 6.

Answer 1.5

The reference for the two-phase multiplier correlation by Murdock should be dated 1962. This reference applies only to the last equation on Page 3-9 of WCAP-8821. You will note in reviewing the reference that the 1.26 in this equation is a multiplier on the  $(1-x_f)$  term and not an exponent as it seems to be in WCAP-8821. This is a typographical error in the WCAP.

The applicability of this and the other correction factors shown on Page 3-9 is discussed in Reference 1 and the Murdock paper. The difference in the exponents on the  $(1-x_f)$  term occur because the equations in the reference are expressed in terms of a friction factor which assumes the total flow is liquid, and those in the WCAP consider only the liquid phase flowing alone in the channel. The relationship between the two factors is defined, using the Blasius equation, as

$$\frac{f}{f_{fo}} = \frac{1}{(1-x_f)^{.25}}$$

### QUESTION 1.6

Special connecting flow paths are discussed in Section 3.3. One of these types is for cross-flow through a regularly spaced tube bundle. Provide the equations and appropriate justification for this type of flow path. Discuss the reasons for the use of this type of flow path in modeling MODEL D steam generators and not MODEL 51 steam generators.

Answer 1.6

The cross-flow correlation used in the TRANFLO code is the following:

$$\Delta p_{\text{fric}} = 1.92 \left( \frac{A_f}{D_H |W|} \right)^{0.2} \left( \frac{12 D_H}{T_p} \right)^{0.4} (\mu)^{0.2} \frac{v_{yx}}{g_c A_f^2 D_H} |W|$$

or 
$$\Delta p_{\text{fric}} = 1.92 \left( \frac{D_H}{T_p} \right)^{0.4} (\text{Re})^{-0.2} \frac{v_{\text{eff}} x}{g_c D_H} |G|$$

where

$D_H$  = hydraulic diameter

$T_p$  = tube pitch

Re = Reynold's number

$v_{\text{eff}}$  = effective specific volume (see Page 3-9 of WCAP-8821)

$x$  = length along flow path

$g_c$  = gravitational constant

$A_f$  = flow area

$G$  = mass flux

This correlation comes from the report "Cooperative Research Program on Shell and Tube Heat Exchangers", by K. J. Bell, University of Delaware Engineering Experimental Station, June 1963.

A cross-flow correlation is needed in the Model D steam generators to represent the flow in the preheater cross-flow paths where the prevailing flow direction is across the tubes rather than along the tubes. In the Model 51 steam generator a cross flow correlation is not needed because the flow direction throughout the tube bundle is parallel to the tubes (see Figure 4.1-1 of WCAP-8821).

The crossflow paths in the Model D computer simulation are those numbered 1, 3, 5, 7, 9, 11, 13, and 15 in Figure 4.2-2a in WCAP-8821. Flow paths 2, 4, 6, 8, 10, 12, 14, and 16 in the preheater region represent flow through the clearance space between the steam generator tubes and the preheater baffle plates.



QUESTION 1.7

Section 3.5 discusses use of the Davis entrainment threshold correlation. Discuss how the de-entrained liquid is transferred between control volumes to the lower regions of the steam generator using this correlation.

### Answer 1.7

The two-phase flow model in TRANFLO does not consider counter-current flow situations. The Davis entrainment threshold is used only to anticipate cocurrent steam/water flows in a vertical direction. As discussed in Section 3.5 of WCAP-8821, a flow test is made in each vertical flow path to determine fluid entrainment. This is done as follows:

1. The calculated flow rate from the matrix solution of the system equations (see Appendix B of WCAP-8821) is assumed to be saturated steam and the flow velocity for steam-only flow is determined using the Davis curve.
2. If the steam-only velocity is below the threshold velocity predicted by Davis, no entrainment is assumed.
3. If the steam-only velocity is greater than 1.8 times the Davis threshold velocity, the Armand correlation is used to predict the flow composition.
4. If the steam-only velocity is between 1.0 and 1.8 times the Davis threshold, a linear transition in flow quality between no entrainment and the Armand predicted value is assumed.

Since the model does not account for counter-current flow situations, it does not transfer liquid from a higher to a lower control volume when the net flow is from the lower to the higher volume. Fluid will be transferred to a lower volume from a higher volume only when the flow direction is calculated to be downward.

QUESTION 1.8

The equation for calculating swirl vane efficiency on page 4-20 is not consistent with the equation on Figure 4.3.1-2a. Please provide the proper equation. The swirl vane efficiency equation appears to be independent of pressure. Discuss the cause of the pressure dependency exhibited in Figure 4.3.1-2b.

Answer 1.8

The equation of Figure 4.3.1-2a is in error. The denominator on the right-hand side of the equation should be  $1.0 - 0.7 (1 - \chi_{a_i})$ . This change makes the equations on Page 4-20 and Figure 4.3.1-2a consistent.

The swirl vane efficiency equation is in terms of inlet and outlet void fraction, and as such is independent of system pressure. For any given inlet void fraction there is only one outlet value. However, the swirl vane inlet and outlet void fractions are related to flow quality via the Armand correlation. Using that correlation, a specific inlet void fraction may be associated with any given inlet quality and pressure. The outlet void fraction from the swirl vanes can then be determined via the efficiency relation, and outlet quality then determined by again applying the Armand relationship. Because of the pressure dependency of the modified Armand correlation (see Question 1.4), the relationship of inlet to outlet quality is also pressure dependent. This magnitude of the dependency is shown in Figure 4.3.1-2b.

QUESTION 1.9

Figure 4.2-2a indicates the direction of flow in the MODEL D steam generator is from the lower tube sheet into the downcomer. Discuss the indicated direction of this flow path in relation to normal operation of the steam generator.

Answer 1.9

The flow direction indicated for flow paths 23 and 25 on Figure 4.2-2a are chosen for convenience to provide mathematical definition to flow direction. During normal operation of the steam generator, the flow in these paths would be opposite of the direction indicated on the drawing. During a large steam break event, however, the flow direction during the early part of the blowdown will be positive, i.e. in the direction shown, and later will return to the reverse, or negative direction.

QUESTION 1.10

Provide the results of nodding sensitivity studies used to select the nodal arrangement for the MODEL 51 and MODEL D steam generator.

## ANSWER 1.10

No nodalization sensitivity studies were performed to select the model arrangements specified in WCAP-8821 for Model 51 and D steam generators. The construction of the steam generators dictates a reasonable nodalization from both an analytical and engineering viewpoint. For example, the tube support plates in the tube region, which are physical barriers to flow, seemed logical choices for nodal limits in this region. Similarly, the deck plates in the upper head of the steam generator were natural choices for defining fluid nodes. Finally, the steam/water separators and drains, and the downcomer, because of their physical construction, were convenient and logical choices for structuring the node model. This philosophy of allowing obvious geometrical and structural aspects of the steam generator define the computer model was applied in the development of both the 51 and D nodal schemes.

Subsequent to the writing of WCAP-8822 some nodalization sensitivity studies have been performed for other purposes. One example is a study performed to support ATWT analyses. In this case models with both eight and twenty-four nodes were used in the steam generator tube bundle to predict heat transfer capability. The results of these studies showed the heat transfer in the steam generator during dryout is essentially unaffected by the noding. A second study was conducted to determine the capability of TRANFLO to do steamline depressurization calculations. In this study 100 feet of steamline was modeled using both 10 and 20 nodes and a depressurization transient was analyzed with each. The results were found to be essentially the same. Although no nodalization sensitivity studies have been performed directly related to WCAP-8822, the results of the two studies mentioned above, we feel, indicate that the results presented in WCAP-8822 would not be effected significantly by changes in the models.



QUESTION 1.11

On page 4-20 the quality of the mass flow in the swirl vane drains is stated to increase linearly for high quality flow entering the swirl vanes. Justify that this assumption is conservative for containment analysis.

Answer 1.11

The original model for the swirl vane drains assumed that the fluid moving through the drains was saturated liquid whenever the flow direction was downward. However, this model often resulted in excessive computational times. The problem resulted from the convergence criterion in the TRANFLO code which limits the maximum time step based on the ratio of the change in mass over one time step to the total mass for the most limiting control volume. In general the limiting node, with the original model, became the upper swirl vane region (nodes 4 or 23 as described in Section 4.1 and 4.2 of WCAP-8821) when the void fraction in this area became large. Because the upper swirl vane volumes are relatively small, forcing the drain flow to be all water when the upper swirl vane volumes are highly voided resulted in a large fraction of the total mass of the region being extracted from the node in one time step. To prevent this, the TRANFLO code would automatically reduce the time step so that the specified convergence criteria was met. Often the reduction resulted in time steps of less than  $10^{-5}$  second.

To eliminate this problem, the drain model was modified such that once the void fraction in the upper swirl vane node reaches a threshold value, steam is also allowed to flow in the drains. The threshold values of void fraction were established as indicated by the following sketch.



Swirl Vane Blade

$$\text{Upper Swirl Vane Volume} = \pi D^2 H / 4$$

$$\text{Threshold Void Fraction} = \left[ \begin{array}{l} \\ \\ \end{array} \right] \text{(a,c)}$$

Once the threshold void is reached, the void fraction propagated through the drain is assumed to increase linearly to 1.0 as the void in the swirl vane approaches 1.0, i.e.  $\alpha_{\text{drain}} = (\alpha_{\text{sv}} - \alpha_{\text{threshold}}) / (1.0 - \alpha_{\text{threshold}})$

Sensitivity studies were conducted to determine if this model change impacted the calculated blowdown results. The studies indicated that impact was minimal as is indicated on the attached figures. The figures show the amount of entrained moisture in two full power blowdowns using both the original and the modified drain models. As can be seen, there is no change in the large break results and only minimal changes to the small break results.

EFFECTS OF SWIRL VANE DRAIN MODEL CHANGE

(a,c)

QUESTION 1.12

Provide and justify the equations used to calculate the centrifugal force that is used in the swirl vane drain head calculations described on page 4-20. Discuss the assumptions made for flow out of the swirl vanes when the swirl vane drains become filled with water.

Answer 1.12

A. The centrifugal force head added to the swirl vane drain is

$$\Delta P_{cf} = \left[ \quad \quad \quad \right] (a,c)$$

where

$R_o$  = swirl vane outer radius

$R_i$  = swirl vane hub radius

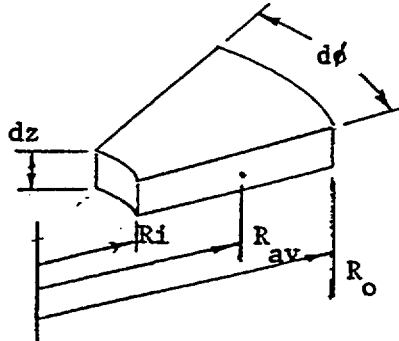
$W$  = drain flow rate

$\beta$  = swirl vane blade angle

$\rho$  = density

$A$  = flow area of drains

The equation is derived by considering an elemental fluid volume as shown



The centrifugal force acting on the  $\phi$ - $z$  surface at  $R_o$  is

$$\left[ \quad \quad \quad \right] (a,c)$$

which is the additional pressure head in the drains due to centrifugal force.

- B. In the TRANFLO steam generator models, the volumes which constitute the swirl vane drains are included as part of the upper downcomer nodes (node 16 for the Model 51 steam generator and node 21 for the Model D steam generator - see Figures 4.1-2a and 4.2-1), and the drain flow is then assumed to go from the inner swirl vane barrel directly into this downcomer volume. Therefore, the "drains", as such, will not fill with water during a transient calculation. The

logic by which the characteristics of flow out of the swirl vanes are determined keys not on the drain volume but on the calculated flows. That is, if the calculated drain flow is from the swirl vanes to the downcomer, the models described on Page 4-20 of WCAP-8821 are used. However, if the flow in the drains is from the downcomer to the swirl vane barrels, the characteristics of the flow out of the swirl vanes will not be corrected to reflect any steam/water separation in the blades. Obviously, with this reverse flow in the drains, any steam/water separation in the blades will be cancelled when the drain mixes with the swirl vane barrel flow at the top of the barrels.



### QUESTION 1.13

Use of the Armand correlation does not appear to be appropriate to predict the quality of steam-water mixtures at high pressures flowing in a vertical direction. The correlation was derived for air-water flow, at atmospheric pressure, flowing in a horizontal direction. The use of horizontal flow data will result in a greater degree of entrainment since the downward gravitational forces on the liquid are not taken into account. This effect is illustrated by the inability of the TRANFLO code to predict the two-phase level measured in Battelle Northwest Test B53B. We believe that the TRANFLO code should be modified to incorporate a two-phase entrainment correlation based on vertical upflow data to replace the Armand correlation. Provide analyses showing the effect of using vertical flow correlations such as those of Wilson and Yeh.

### Answer 1.13

Though originally developed from horizontal, two-phase flow experiments, the Armand correlation has been shown to be an adequate empirical correlation for use in vertical flow situations. The ability of the correlation to predict both two-phase pressure drops and void fractions in vertical flow channels can be verified by review of references 2, 4, 5, 6, and 7.

In particular, Reference 2 demonstrates, using data from Reference 5 and 6, that the Armand correlation of void fraction gives good agreement with experimental data for vertical flow over a wide pressure range for both adiabatic and diabatic situations. Additionally, Reference 2 indicates that in the pressure range of 100 - 600 psia with heat addition, the Armand correlation generally overpredicts void fraction. This particular situation, i.e. pressures around 600 psia accompanied by heat addition, is very characteristic of steam generators during blowdown. Thus use of the Armand correlation will result in higher mass fraction of steam being calculated to rise through the steam generator tubes and less liquid being carried to the top of the steam generator where it may exit in the blowdown.

The adequacy of the Armand correlation to predict two-phase pressure drops is also addressed in the above references as well as in Reference 7, and is generally found to be acceptable in comparison with other well-known correlations. It is important to note that Reference 7 also indicates that, for ranges of data typical of boiling water reactors, the Armand pressure drop correlation resulted in the least rms error from measured data when the entire range of data variation was considered. Again the operating conditions in a BWR are very similar to those in the steam generator of a pressurized water reactor.

The Armand correlation has also been used satisfactorily by others to evaluate voiding in two-phase vertical flow situations (Reference 1) as well as to define the distribution parameter in calculations using the drift flux correlation of Zuber and Wallis (Reference 12). The success

of these efforts, along with the results presented in the referenced papers, we feel is sufficient justification for using the Armand correlation in a vertical flow geometry.

Concerning the Battelle 53B test, we agree that Wilson's or Yeh's correlation might provide better results for this particular test due to the low phase velocities, but we do not agree that they are appropriate for steam line break analyses. The phase velocities expected are much higher than those used by either Wilson or Yeh to develop their results. In fact, if either correlation is applied to conditions typical of those occurring in the steam generator tubes during the first 20 - 30 seconds of a large steam line break, they will generally predict void fractions greater than 1.0.

QUESTION 1.14

To provide an upper limit on the effect on the swirl vanes in increasing the break quality, extend the sensitivity study presented in Figures 5.3.2-1a, b and c to include analyses for a swirl vane efficiency of 100%.

Answer 1.14

The attached figures provide a graphical illustration of the effects of swirl vane efficiency on break quality for the three breaks presented in Figures 5.3.2-1a, b, and c of WCAP-8821. As should be expected, the effects on large breaks are negligible while the effects on small breaks are important with the importance being more pronounced at higher power levels.

ENTRAINMENT SENSITIVITY TO  $n_{sv}$

QUALITY OF BREAK EFFLUENT

(a,c)

BREAK QUALITY VS. TIME FOR A 0.7 FT<sup>2</sup> DER AT 102% POWER

ENTRAINMENT SENSITIVITY TO  $n_{sv}$

QUALITY OF BREAK EFFLUENT

(a,c)

BREAK QUALITY VS. TIME FOR A 0.7 FT<sup>2</sup> DER AT 102% POWER

ENTRAINMENT SENSITIVITY TO  $n_{sv}$

(a,c)

QUALITY OF BREAK EFFLUENT

BREAK QUALITY VS. TIME FOR A 0.5 FT<sup>2</sup> DER AT 30% POWER



ENTRAINMENT SENSITIVITY TO  $\eta_{sv}$

QUALITY OF BREAK EFFLUENT

(a,c)

BREAK QUALITY VS. TIME FOR A 1.4 FT<sup>2</sup> DER AT 102% POWER

### QUESTION 1.15

The sensitivity study presented in Figures 5.3.2-1a, b and c indicates that the quality leaving the break is relatively insensitive to assumed values of swirl vane separation efficiency. These results do not appear to be consistent with the comparisons presented in Figures 5.3.2-6, 7 and 8, which exhibit a large sensitivity to swirl vane efficiency predicted by the Steady State Experimental Model. Discuss the reasons for this apparent inconsistency. Provide the empirical correlations discussed on page 5-46 used to generate the comparison with the computer model and discuss the differences between these correlations and the TRANFLO correlation presented on page 4-20. Discuss which empirical correlation was used for each comparison.

Answer 1.15

Figures 5.3.2-1a, b, c are not inconsistent with Figures 5.3.2-6, 7, 8. Figures 5.3.2-1a, b, c are intended to illustrate the insensitivity of the blowdown entrainment to the value used for  $\eta_{sv}$  in the swirl vane model described on Page 4-20. Figures 5.3.2-6, 7, 8 are intended to show the conservative margin between blowdown quality calculated using the model described on Page 4-20 (with  $\eta_{sv}=0.7$ ) and the blowdown quality predicted when the model described by Figures 5.3.2-4 and 5.3.2-5 is used.

Stated differently, Figures 5.3.2-1a, b, c indicate that the value chosen for  $\eta_{sv}$  in the standard TRANFLO swirl vane model has little impact on the entrainment that results. This model was used to generate the blowdowns which were used to develop the data presented in Appendix A of WCAP-8822. Figures 5.3.2-6, 7, 8 are only used to illustrate that, were the model used in TRANFLO developed from steady-state separator data, the entrainment calculated to result from the blowdown would be much greater. Thus, from the viewpoint of specific energy of the effluent, the standard swirl vane model gives conservative results for containment analyses.

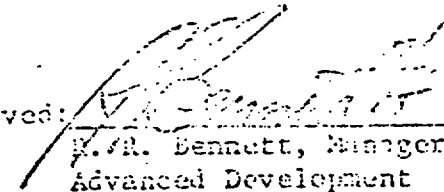
TRANFLO Versus Experimental Swirl Vane Model

The experimental correlation discussed on Page 5-46 is explained in the attached report, "Moisture Carryover Calculation Procedure", by A. W. Bjorkedal. As indicated, the steam generator data used in the development of the correlation is from Model 44 and Model 51 steam generators at numerous Westinghouse plants. The orifice to blade tip diameter ratios for these plants were [ ] Differences between this approach to modeling separator performance and the TRANFLO model can be understood by comparing this report with Sections 4.3.1 and 4.3.2 of WCAP-8821.

(a,c)

The comparisons shown on Figures 5.3.2-2, 3, 6, 7, 8 and the separator performance curves shown in Figures 5.3.2-4, 5 are all derived from the attached report. The data points shown on Figure 5.3.2-2 are derived from the circulation ratios and the values of swirl vane exit quality reported

in the data tables. The modified Armand correlation was used to convert quality values to values of void fraction. Data points on Figure 5.3.2-3 were derived by substituting the values for swirl vane inlet and outlet void fraction from Figure 5.3.2-2 into the TRANFLO swirl vane equation shown on Page 4-20 and determining  $\eta_{sv}$ . Figures 5.2.2-4 and 5 are simple parametric plots of the equations presented in the report. A value of orifice to tip diameter of [ ] was used to generate these curves since (a,c) it closely matches the value of [ ] for Model D swirl vanes. Figures 5.3.2-6, 7, and 8, as explained earlier, simply compare the calculated blowdown results for a selection of postulated steam line breaks using first, the TRANFLO model and second, the equations from the attached report to specify separator effectiveness. A value of orifice to tip diameter ratio of [ ] was used for these comparisons also. (a,c)

Approved: 

E. R. Bennett, Manager  
Advanced Development

Moisture Carryover Calculation Procedure

By: A. W. Bjorkedal

June 1975

Westinghouse Electric Corporation

Tampa Division

Tampa, Florida

Reviewers Summary

Report Title: Moisture Carryover Calculation Procedure  
Report Number: WTD-AD-75-025  
Report Date: June 1975  
Author's Name: A. W. Bjorkedal  
Reviewer's Name: R. R. Bennett

Nature of Report: Documentation of Prediction Method for Moisture Carryover

Specific Product Applicability: All D & S Steam Generators, steam drums for non nuclear application

Is analysis complete and accurate? Yes

Have the results been supported by alternate calculations? No

If not, state why? Supported by experimental data

Are related significant findings by others summarized? No

If not, state why? New technique

State source of supporting experimental or operating data not included.

Significant supporting data included

  
Author's Signature

  
Reviewer's Signature

July 31, 1975

Date

## Table of Contents

	<u>Page</u>
Nomenclature	1
Introduction	2
Theory	3
Appendix A - Sample Calculations	7
Appendix B - Figures	10
Appendix C - Data	20

### Nomenclature

$A_{sv}$	=	Swirl vane flow area, $ft^2$
$A_{up}$	=	Secondary separator upflow area, $ft^2$
CR	=	Circulation ratio
$D_h$	=	Swirl vane hub diameter, in.
$D_t$	=	Swirl vane tip diameter, in.
NR	=	Number of risers
ORF	=	Orifice factor
ORFE	=	Orifice efficiency factor
$P_s$	=	Steam pressure, psia
$P_{vg}$	=	Secondary separator upflow dynamic head, psi
$V_{liq}$	=	Swirl vane liquid velocity, ft/sec
$V_{lmin}$	=	Minimum swirl vane liquid velocity, ft/sec
$V_{up}$	=	Secondary separator upflow velocity, ft/sec
$v_g$	=	Specific volume saturated vapor, $ft^3/lbm$
$v_l$	=	Specific volume saturated liquid, $ft^3/lbm$
$W_s$	=	Steam flow, $lbm/hr$
$X_a$	=	Void fraction into primary separators
$X_m$	=	Steam quality into primary separators
$X_s$	=	Steam quality into secondary separators
$\gamma$	=	Slip factor
$\Delta E_{act}$	=	Actual vapor - liquid energy difference
$\Delta E_{min}$	=	Minimum vapor - liquid energy difference
$\eta_a$	=	Actual primary separator efficiency
$\eta_{cor}$	=	Corrected primary separator efficiency
$\eta_n$	=	Normalized primary separator efficiency
$\eta_{pre}$	=	Preliminary primary separator efficiency
$\rho_g$	=	Density saturated vapor, $lbm/ft^3$
$\rho_l$	=	Density saturated liquid, $lbm/ft^3$



## Introduction

Separator performance tests have been conducted both in the laboratory and in the field. These tests have provided moisture carryover data as a function of the secondary side operating parameters. Employing an approach which considers the vapor and liquid phases of the flow separately, a moisture carryover prediction method which accurately predicts separator performance has been developed. The following pages delineate this method. A sample calculation is included in Appendix A.

## Theory

Early efforts in analyzing moisture separator performance concentrated on the average fluid properties of the liquid-vapor flow. For the second-stage separators, this approach yields accurate results. However, for the swirl vane separators, an approach considering the vapor and liquid phases separately has greatly improved separator analysis.

To consider the vapor and liquid phases separately, a model for void fraction and slip ratio must be selected. Thom's model is used due to its ease of application. Thom's model specifies that at any given pressure, the slip ratio and the slip factor are constant. Value of slip factor are given in Table 1.

Table 1  
Slip Factor Vs. Pressure

Pressure, psia	14.7	250	600	1250	2100	3000	3206
Slip Factor	246	40.0	20.0	9.80	4.95	2.15	1.00

These points can be fitted to a curve defined by:

$$\begin{aligned} \gamma = & \exp (5.732629 - 1.92757075 \times 10^{-2} (P_S) + \\ & 7.50059652 \times 10^{-5} (P_S)^2 - 1.65676214 \times 10^{-7} (P_S)^3 + \\ & 1.96115024 \times 10^{-10} (P_S)^4 - 1.16849286 \times 10^{-13} (P_S)^5 + \\ & 2.74824248 \times 10^{-17} (P_S)^6) \end{aligned}$$

This curve is plotted on Figure 1.

Knowing the circulation ratio of the steam generator, the quality of the flow leaving the tube bundle and entering the primary separator can be determined by:

$$X_m = \frac{1}{CR}$$

With the slip factor and the quality into the primary separator known, the void fraction of the flow into the primary separator can be determined by:

$$X_a = \frac{(\gamma) (X_m)}{1 + (\gamma - 1) (X_m)}$$

After determining the swirl vane flow area,

$$A_{sv} = \frac{(D_t^2 - D_h^2) (\pi R) (\pi)}{576}$$

The liquid velocity into the swirl vane can be determined:

$$V_{liq} = \frac{(1 - X_m) (W_s) (V_1)}{(1 - X_a) (A_{sv}) (X_m) (3600)}$$

Knowing the flow conditions into the primary separators, the efficiency of the separators must be determined.

Efficiency is defined as water removed divided by water entering. Field and laboratory data were reviewed to determine what combination of performance parameters would cause the efficiency curves at 200 psia and 500 psia to coincide. Of the terms investigated, only the momentum difference and the energy difference terms accomplished the desired effect. Energy difference is defined as:

$$\Delta E = \rho_l V_l^2 - \rho_g V_g^2$$

The liquid and vapor velocities can be related by:

$$V_g = s V_l, \text{ where } s = \text{slip ratio} = \frac{\rho_l}{\rho_g \gamma}$$

Thus,

$$\Delta E = (\rho_l - \rho_g \left(\frac{\rho_l}{\rho_g \gamma}\right)^2) V_l^2, \text{ or}$$

$$\Delta E = (\text{density difference}) (\text{liquid velocity})^2$$

The density difference term of the liquid and vapor phases can be defined by:

$$D = \rho_l - \rho_g \left(\frac{\rho_l}{\rho_g \gamma}\right)^2$$

Since densities of the vapor-liquid phases vary solely as a function of pressure, a D/D200 ratio can be defined as a function of pressure, where:

$$D_{200} = \text{density difference at 200 psia} = 50 \text{ lb/ft}^2$$

$$P = \text{density difference at } P_g, \text{ psia}$$

$$\begin{aligned} D/D_{200} &= 1.10962495 - (3.86208791 \times 10^{-4}) (P_g) \\ &\quad + (7.63413057 \times 10^{-8}) (P_g)^2 \end{aligned}$$

This ratio is plotted on Figure 2.

Thus the actual energy difference can be determined by:

$$\begin{aligned}\Delta E_{\text{act}} &= (\text{density difference}) (\text{liquid velocity})^2 \\ &= (50) (D/D200) (V_1)^2\end{aligned}$$

The test data was reviewed to determine a normalized separator efficiency at 200 psia. It was found that a minimum liquid velocity into the primary separators could be defined as a function of void fraction:

$$\begin{aligned}V_{1\text{min}} &= \exp (-1.63506342 \times 10^1 + 1.38683516 \times 10^2 (x_a) \\ &\quad - 4.53364597 \times 10^2 (x_a)^2 + 7.42282031 \times 10^2 (x_a)^3 \\ &\quad - 5.97630475 \times 10^2 (x_a)^4 + 1.89936449 \times 10^2 (x_a)^5), \\ &\quad \text{plotted on Figure 3.}\end{aligned}$$

From this value, a minimum energy difference can be determined:

$$\begin{aligned}\Delta E_{\text{min}} &= -3.839976 - 1.1335 (V_{1\text{min}}) + 0.60088 \times 10^2 (V_{1\text{min}})^2 \\ &\quad - 0.41024 \times 10^1 (V_{1\text{min}})^3 + 0.45988 (V_{1\text{min}})^4 - 0.18828 \times 10^{-1} \\ &\quad (V_{1\text{min}})^5 + 0.24690 \times 10^{-3} (V_{1\text{min}})^6\end{aligned}$$

This curve is plotted on Figure 4.

The normalized primary separator efficiency is then given as a function of  $\Delta E_{\text{min}}$ :

$$\begin{aligned}\eta_n &= 1.0 - 0.16209 \times 10^{-4} (\Delta E_{\text{min}}) + 0.25513 \times 10^{-7} (\Delta E_{\text{min}})^2 \\ &\quad - 0.11782 \times 10^{-10} (\Delta E_{\text{min}})^3 + 0.18616 \times 10^{-14} (\Delta E_{\text{min}})^4 \\ &\quad - 0.11761 \times 10^{-18} (\Delta E_{\text{min}})^5 + 0.24673 \times 10^{-23} (\Delta E_{\text{min}})^6\end{aligned}$$

for  $\Delta E_{\text{min}} < 10000$ ;

for  $\Delta E_{\text{min}} \geq 10000$ ,  $\eta_r = 0.93$

$\eta_n$  is plotted on Figure 5.

From these factors, a preliminary primary separator efficiency can be determined based on the pressure and velocity terms.

$$\eta_{\text{pre}} = f (\text{pressure effects}) f (\text{velocity effects})$$

$$\eta_{\text{pre}} = (D/D200) (\eta_n) \text{ where } \Delta E_{\text{act}} \geq \Delta E_{\text{min}}$$

or

$$\eta_{\text{pre}} = (D/D200) (\eta_n \times \frac{\Delta E_{\text{act}}}{\Delta E_{\text{min}}}) \text{ where } \Delta E_{\text{act}} < \Delta E_{\text{min}}.$$

All of these calculations have been based on primary separators with orifice to tip diameter ratios of 0.85. For primary separators with orifice to tip diameter ratios of less than 0.85, a correction factor must be applied to the separator efficiency. This correction factor varies both with primary separator liquid velocity and with diameter ratio.

$$\text{ORFE} = 1.0 + (\text{ORF} - 1.0) \left(\frac{V_{\text{lig}}}{8.5}\right)$$

where ORF = 1.20 for a 0.6 diameter ratio,  
 ORF = 1.08 for a 0.7 diameter ratio,  
 ORF = 1.0 for a 0.85 diameter ratio.

Thus, the primary separator efficiency is corrected by:

$$\eta_{cor} = (ORFE) (\eta_{pre})$$

In reviewing field data, it was determined that moisture carryover could be more accurately predicted using the following definition for actual primary separator efficiency:

$$\eta_a = (\eta_{cor}) \left(1.0 - \frac{CR - 3.5}{3.5}\right)$$

Using this separator efficiency, the quality of the flow leaving the primary separator can be determined by:

$$X_s = \frac{1.0}{1.0 + (1.0 - \eta_a) (CR - 1)}$$

Knowing the quality leaving the primary separators, the inlet quality into the secondary separators is assumed to be the same. In order to predict secondary separator performance, the performance of the various secondary separators was defined by a family of curves of moisture carryover versus upflow dynamic head (based on vapor) for various approach qualities. These curves are given on Figures 6 thru 9, Figure 6 for the single-tier separator with peerless vanes, Figure 7 for the two-tier separator with peerless vanes, Figure 8 for the two-tier separator with formed vanes and Figure 9 for the two-tier separator with formed vanes and perforated plates.

Knowing the secondary separator upflow area, the upflow velocity can be determined by:

$$V_{up} = \frac{(W_s) (v_g)}{(A_{up}) (3600)}$$

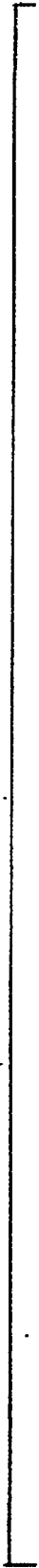
and the upflow dynamic head by:

$$P_{vg} = \frac{(V_{up})^2}{(64.36) (144) (v_g)}$$

Entering the appropriate figure with  $P_{vg}$  and  $X_s$ , the expected moisture carryover can be extracted.

Appendix A  
Sample Calculation

(a,c)



(a.c)





Appendix B

Figures

Figure 1  
Slip Factor  
vs.  
Pressure

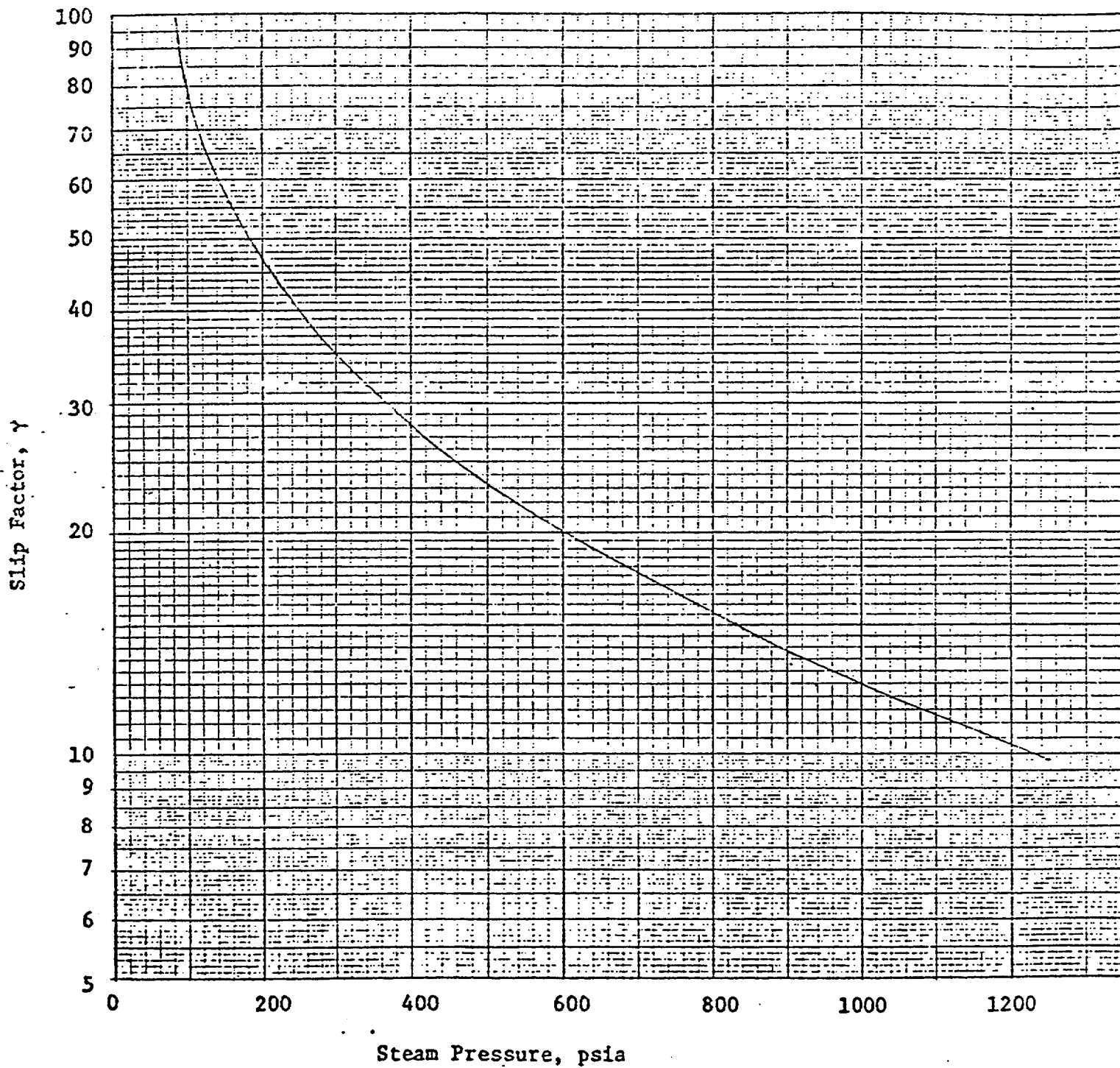


Figure 2

$D/D_{200}$

vs.

$P_s$

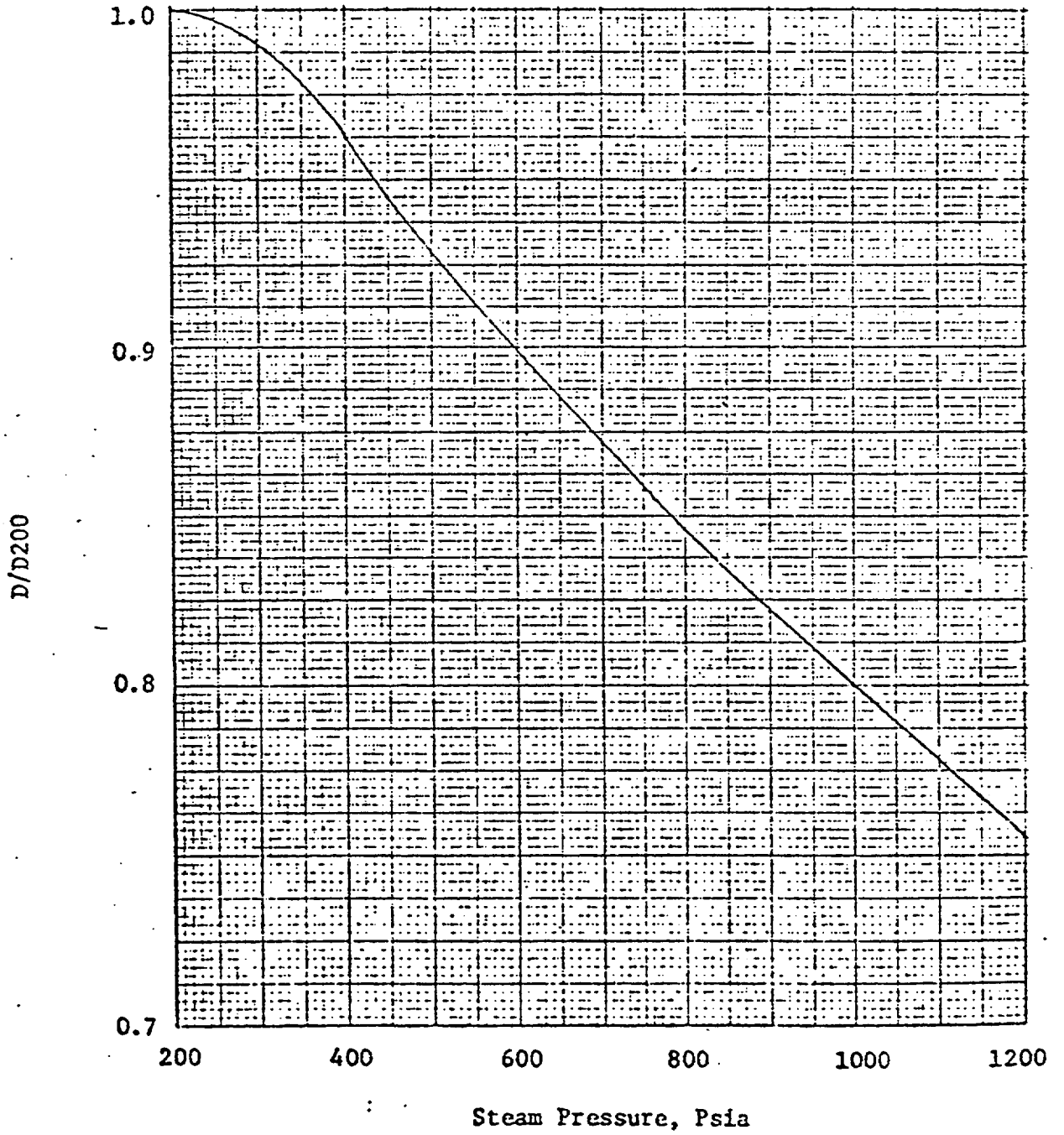
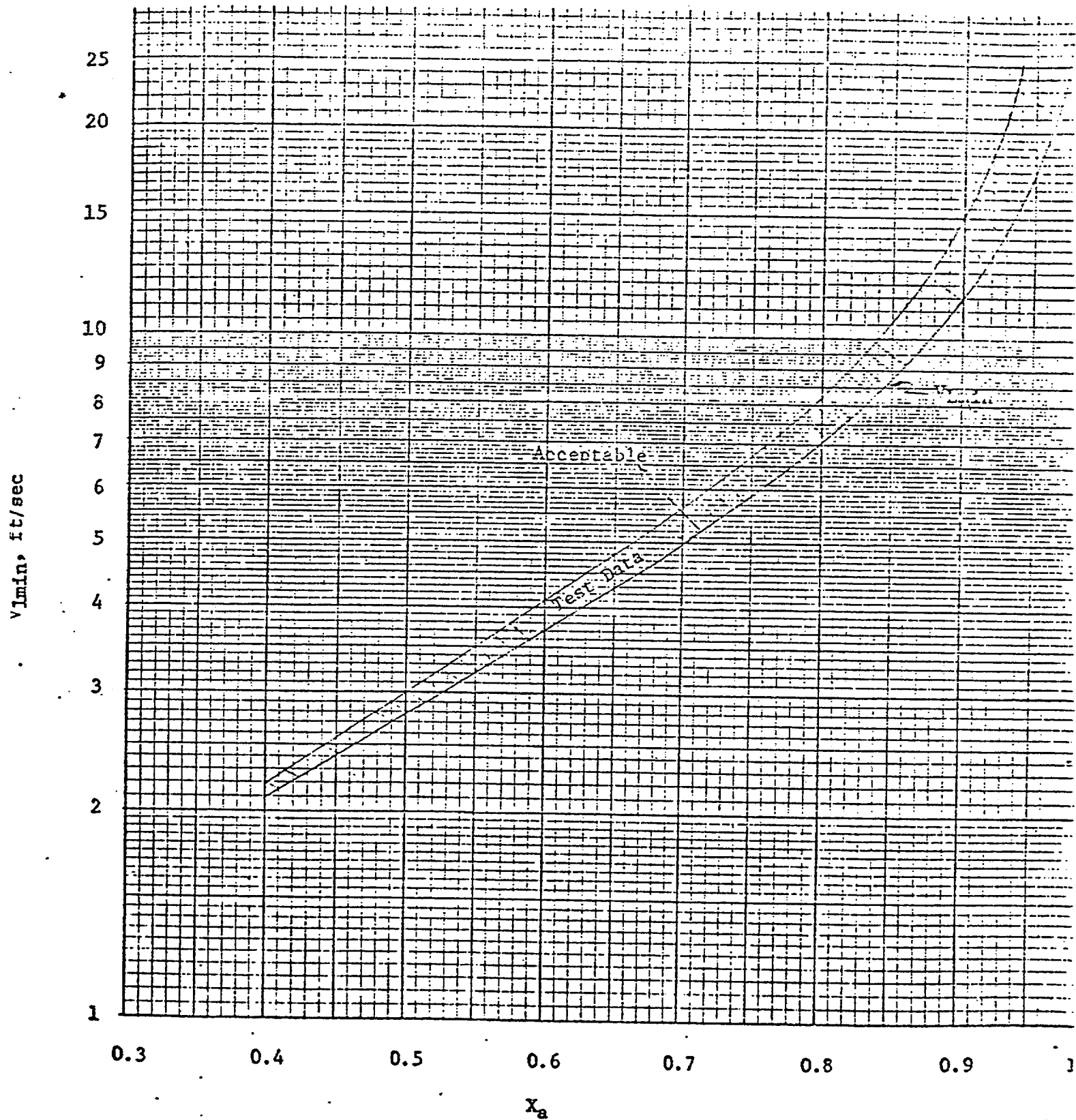


Figure 3

$V_{min}$   
vs.  
 $X_a$



$V_{lim}$ , ft/sec

30

25

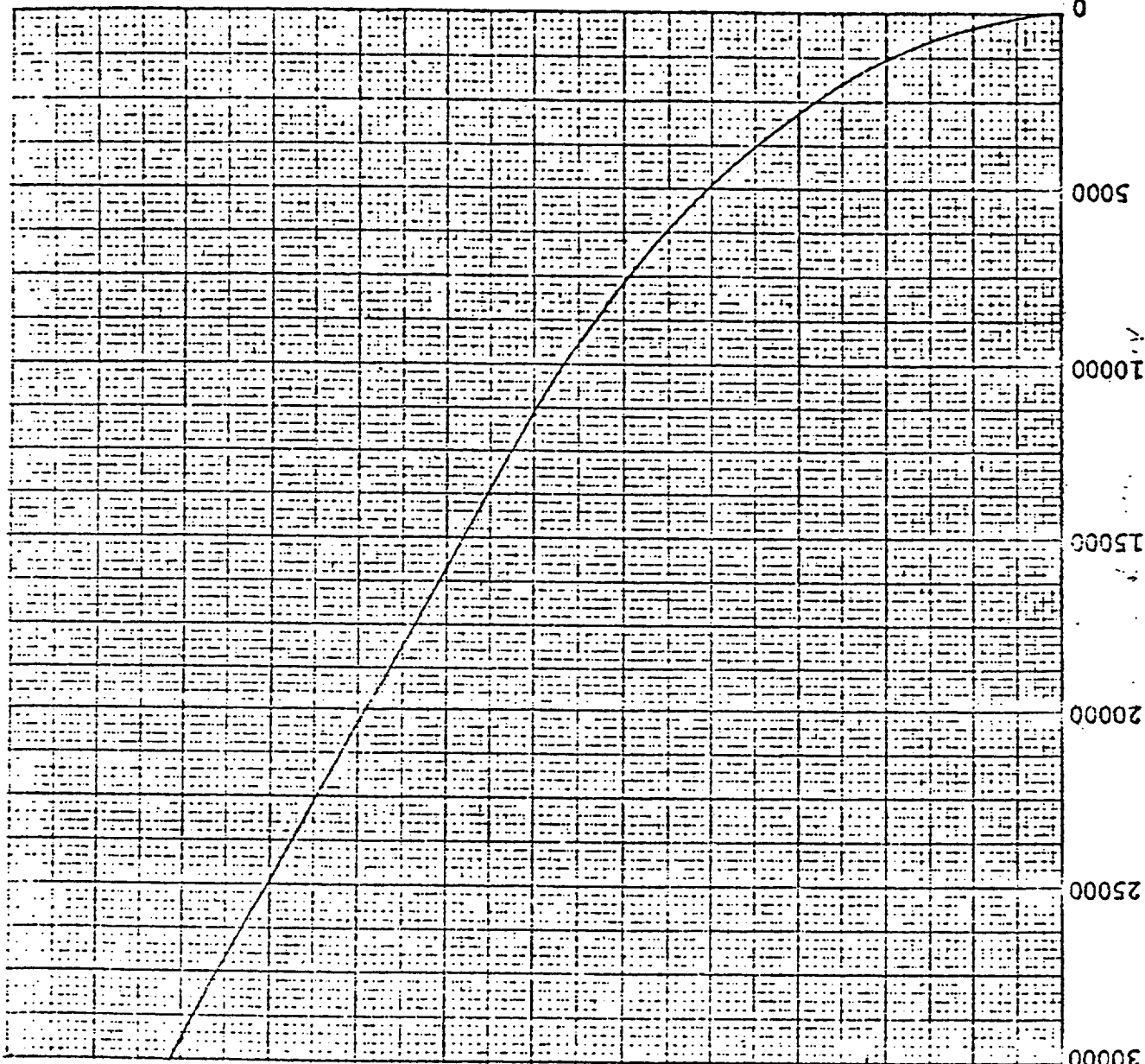
20

15

10

5

0



$\Delta E_m$ , lb/ft<sup>2</sup>-sec<sup>2</sup>

$V_{lim}$

30

$\Delta E_m$

Figure 4

Figure 5

$\eta_a$

vs

$\Delta E_{min}$

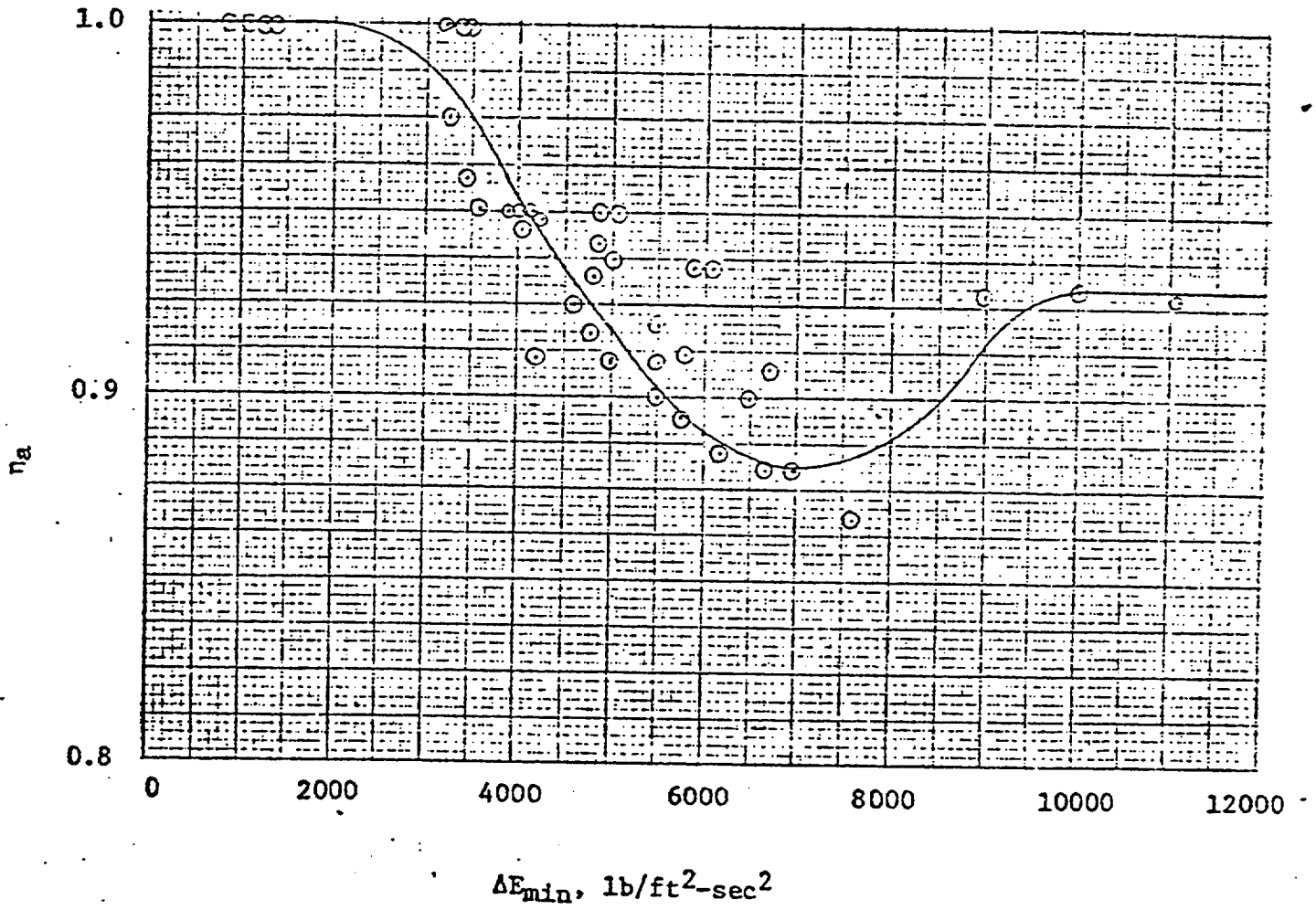


Figure 6  
Single-Tier - Peerless  
Moisture Carryover  
vs.  
Upflow Dynamic Head

(a,c)

Moisture Carryover, %

Upflow Dynamic Head, psi

For Data, see Appendix C

Figure 7  
Two-Tier - Peerless  
Moisture Carryover  
VS.  
Upflow Dyanmic Head

(a,c)

MOISTURE CARRYOVER, %

Upflow Dyanmic Head, psi

For Data, see Appendix C



Two-Tier Formed  
Moisture Carryover  
vs.  
Upflow Dynamic Head

Figure 8

(a,c)

Upflow Dynamic Head, psi

Two-Tier Formed with Perforated Plate

Figure 9      Moisture Carryover  
                                 vs.  
                                 Upflow Dynamic Head

(a,c)

Upflow Dynamic Head, psi

Appendix C

Data

TABLE 1  
Single Tier Peerless Data

(a,c)

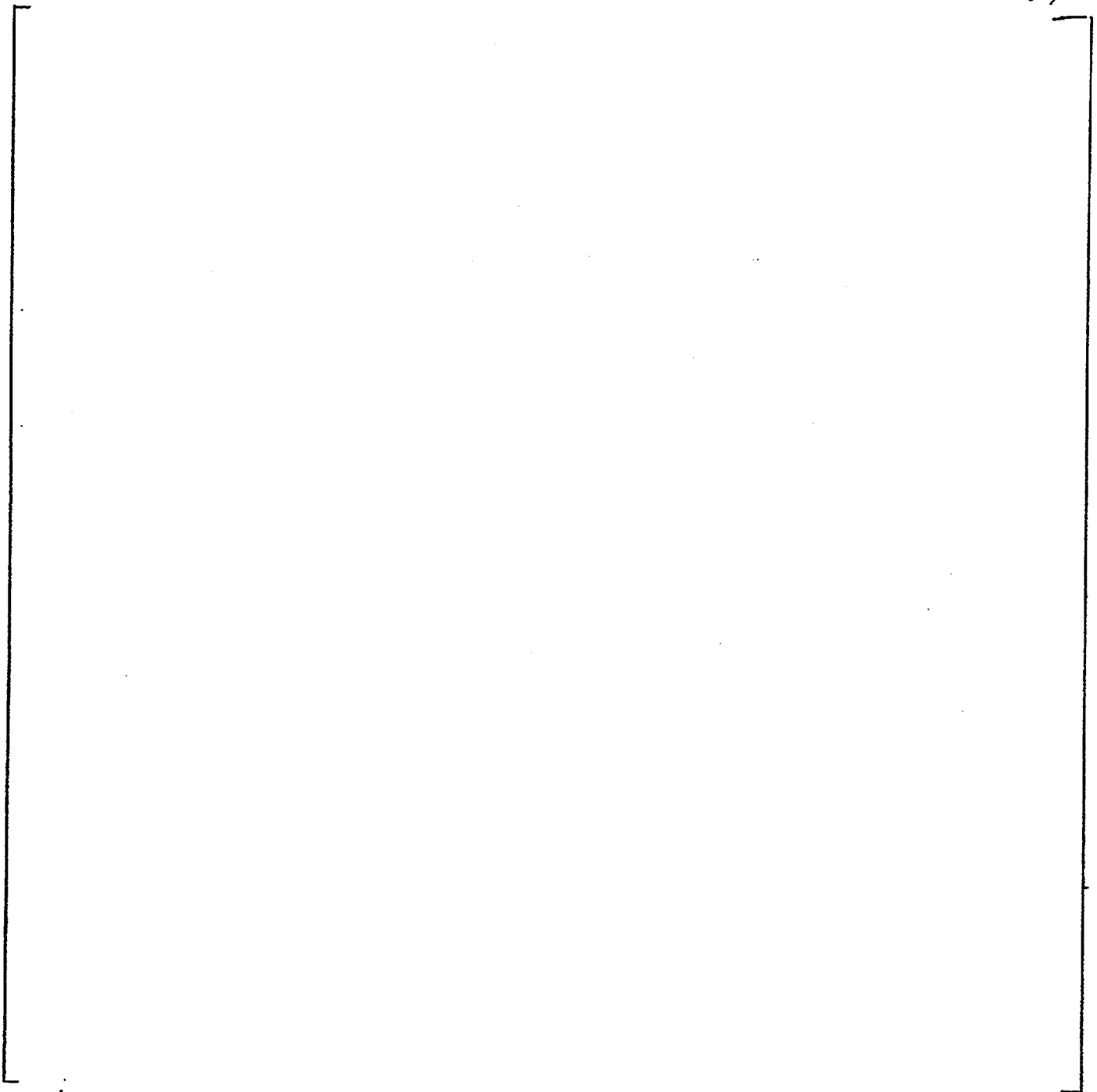


TABLE 1 - Continued

(a,c)

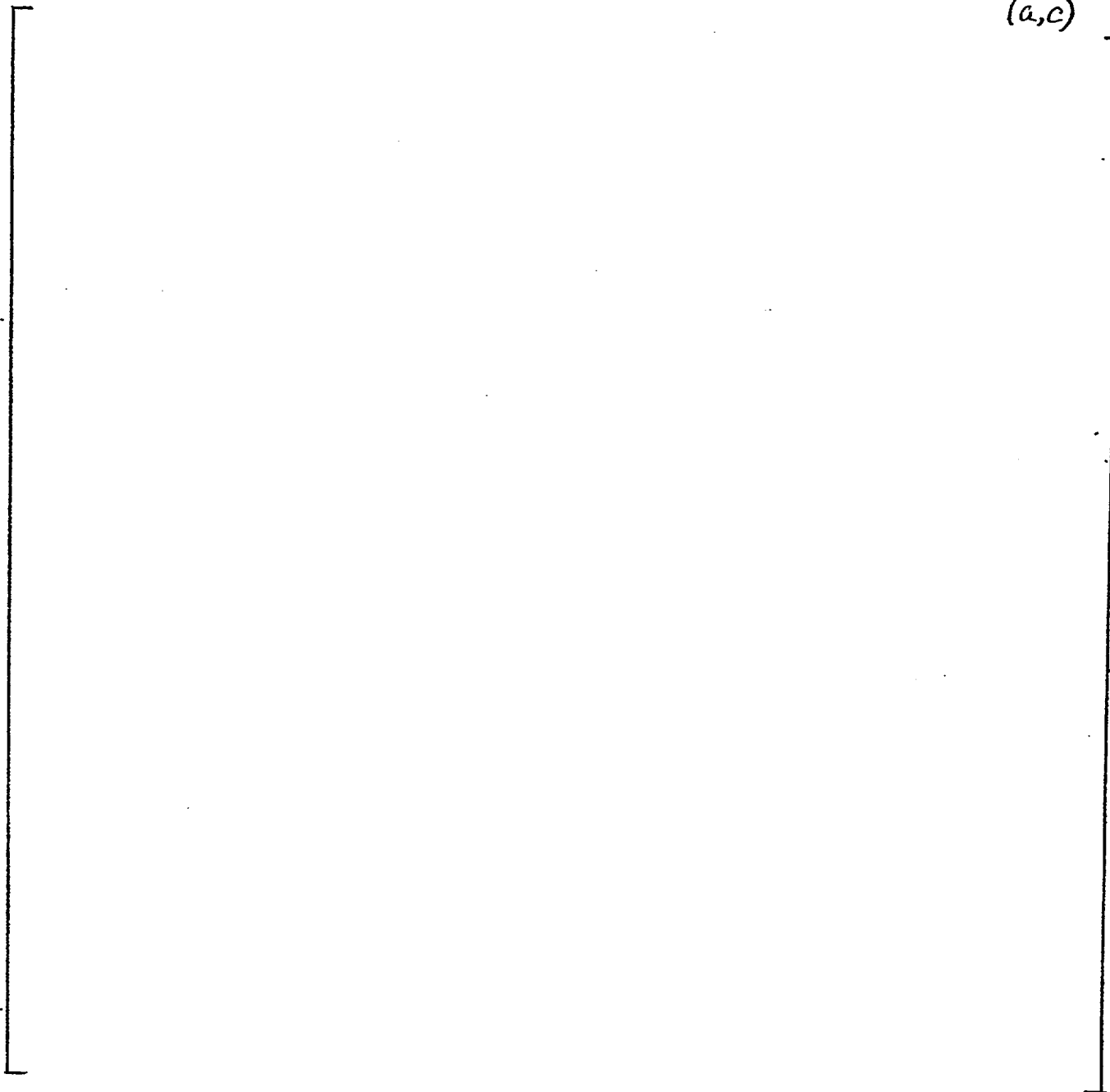
A large, empty rectangular frame with a thin black border, occupying most of the page. It appears to be a placeholder for a table or data that is not present in this scan.

TABLE 2  
Two Tier Peerless Vanes

(a,c)

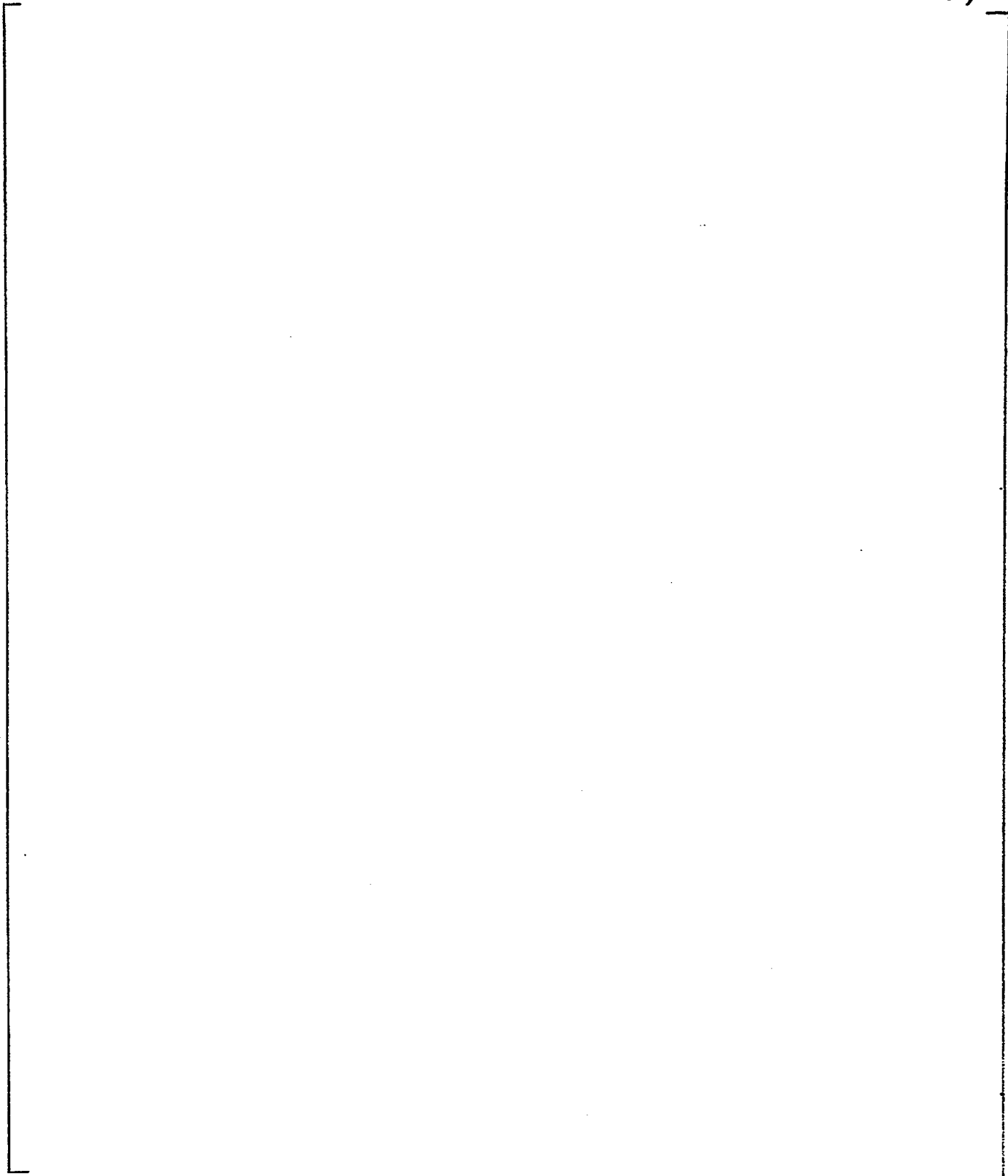


TABLE 3  
Two Tier Formed Vanes

(a,c)

A large, empty rectangular frame with a thin black border, spanning most of the page's width and height. It appears to be a placeholder for a table or diagram.

TABLE 4

Two Tier Formed Vanes with Perforated Plates

(a,c)

A large, empty rectangular frame with a thin black border, spanning most of the width and height of the page. It appears to be a placeholder for a table or diagram.



QUESTION 1.16

Describe the test program used to obtain the separation efficiency for the swirl vanes in operating steam generators discussed on page 5-41 and 5-46. Provide the test procedure and discuss the instrumentation used to monitor significant parameters. There appear to be two types of swirl vane separators in Westinghouse plants; those for the MODEL 51 steam generator and a smaller version used in the MODEL D steam generator. For each test, indicate which type of separator was being tested. Justify that data for the MODEL 51 separators are applicable for the MODEL D separators.

Answer 1.16

The procedures and test instrumentation used to determine the steady-state separator efficiency of operating steam generators is described in the attached report. These procedures are consistent with accepted industry practices for measuring carry-over in steam drying and generation equipment.

A description of the type of swirl vanes for which the test data exists is given in the answer to question 1.15. The applicability of the data to Model D type separators is based on the fact that range of orifice-to-tip diameter ratios covered by the correlations includes the orifice-to-tip diameter ratio of the Model D swirl vanes.

Approved.

R. P. Wedler 5/17/72

R. P. Wedler, Manager  
Pressurized Water  
Equipment Engineering

General Procedure for Determining the  
Moisture Carryover Performance of the 51 Series Steam Generators  
in a 3 Loop Pressurized Water Nuclear Plant

by

Albert W. Bjorkedal

May, 1972

Westinghouse Electric Corporation  
Tampa Division  
Tampa, Florida

## TABLE OF CONTENTS

	<u>Page</u>
Nomenclature	
1.0 Introduction	1
2.0 Theory	2
2.1 Derivation of Equations	2
2.2 Sampling Points	7
2.3 Circulating Water Sample	8
2.3.1 Bottom Blowdown	8
2.4 Recirculating Water Sample	8
2.4.1 Steam Drum Sampling Tap	8
2.5 Steam Sample	9
2.5.1 Steam Probe	9
2.5.2 Feedwater Pump Discharge Piping	10
2.5.3 Condenser Hotwell	10
3.0 Sampling Procedure	10
3.1 Water Chemistry	10
3.2 Steam Generator Preparation	11
3.3. Sampling Apparatus	11
3.4 Sampling Technique	12
3.5 Sampling Rates	13
3.6 Sample Analysis	13
3.7 Data	14
3.8 Final Adjustment of Steam Generator Chemistry	14
4.0 Calculation Procedure	15
5.0 References	20

## Nomenclature

- $C_b$  = Sodium concentration of bottom blowdown water sample
- $C_{ba}$  = Sodium concentration of bottom blowdown in Loop A
- $C_{bb}$  = Sodium concentration of bottom blowdown in Loop B
- $C_{bc}$  = Sodium concentration of bottom blowdown in Loop C
- $C_{f1}$  = Sodium concentration of feedwater from pump number 1
- $C_{f2}$  = Sodium concentration of feedwater from pump number 2
- $C_{f3}$  = Sodium concentration of feedwater from pump number 3
- $C_s$  = Sodium concentration of condenser steam sample
- $C_t$  = Sodium concentration of steam drum tap sample
- $C_{ta}$  = Sodium concentration of tap sample in Loop A
- $C_{tb}$  = Sodium concentration of tap sample in Loop B
- $C_{tc}$  = Sodium concentration of tap sample in Loop C
- $CO$  = Moisture carryover
- $\overline{CO}$  = Average moisture carryover
- $CO_a$  = Moisture carryover of Loop A
- $CO_b$  = Moisture carryover of Loop B
- $CO_c$  = Moisture carryover of Loop C
- $C_{sa}$  = Sodium concentration of steam probe in Loop A
- $C_{sb}$  = Sodium concentration of steam probe in Loop B
- $C_{sc}$  = Sodium concentration of steam probe in Loop C
- $CR$  = Circulation ratio
- $\Sigma N_a$  = Total sodium ion in steam
- $P_s$  = Steam pressure

Nomenclature (Cont'd)

- $n$  = Number of feedwater pumps
- $TFW$  = Feedwater temperature
- $WFW$  = Feedwater flow rate
- $WFW_a$  = Feedwater flow rate of Loop A
- $WFW_b$  = Feedwater flow rate of Loop B
- $WFW_c$  = Feedwater flow rate of Loop C
- $W_s$  = Steam flow rate
- $W_{sa}$  = Steam flow rate of Loop A
- $W_{sb}$  = Steam flow rate of Loop B
- $W_{sc}$  = Steam flow rate of Loop C

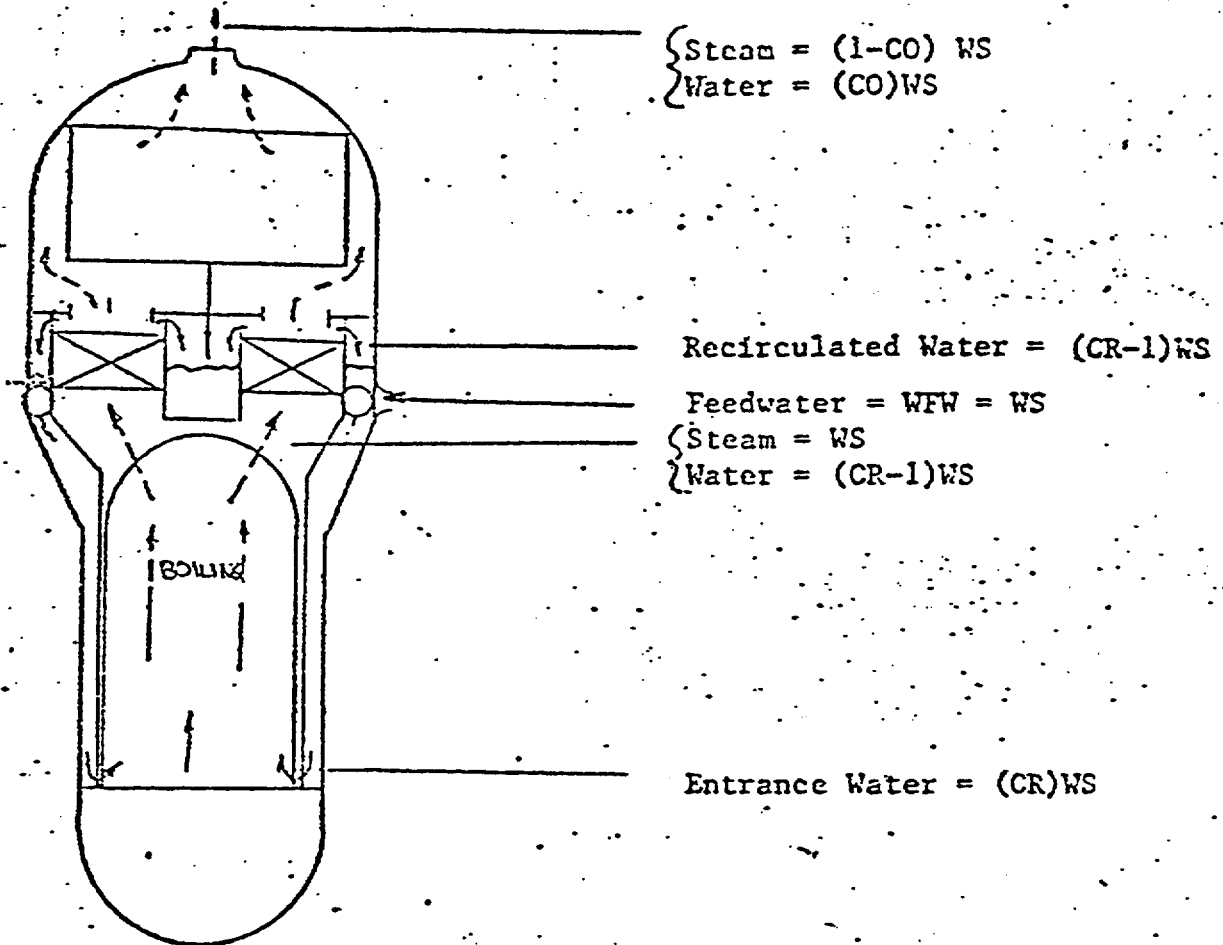
## 1.0 Introduction

Westinghouse Electric Corporation's Tampa Division has adopted the sodium tracer technique as the most accurate method of determining moisture carryover performance of a steam generator. Under this technique, sodium is added to the steam generator in the form of sodium phosphates which dissolve in the circulating water and remain dissolved in the water carried out of the vessel by the steam. The moisture carryover can be computed from sodium concentration of the steam and recirculating water. The sodium concentrations are determined from the analysis of water samples by flame spectrometry. The methods presented in this procedure are considered the most advanced techniques in the industry.

The procedure delineated in this report has been prepared specifically for use at a 3 loop pressurized water nuclear plant using 51 series steam generators. This is a general procedure which includes use of steam probes and an unspecified number of pumps.

## 2.0 Theory

### 2.1 Derivation of Equations



The moisture carryover is determined from the dilution of the sodium concentration of the steam sample due to the steam condensing. Since the total mass of the dissolved sodium remains constant, the carryover equation is derived by a mass balance.

The carryover is defined as:

$$CO \equiv \frac{\text{water mass in steam}}{\text{total steam mass}}$$

The mass of water present in the steam =  $(CO)(W_s)$

The mass of sodium in the moisture =  $\sum N_{a_m} = C_l (CO)(W_s)$

The mass of sodium in condensed steam sample =  $\sum N_{a_s} = C_s (W_s)$



By a mass balance

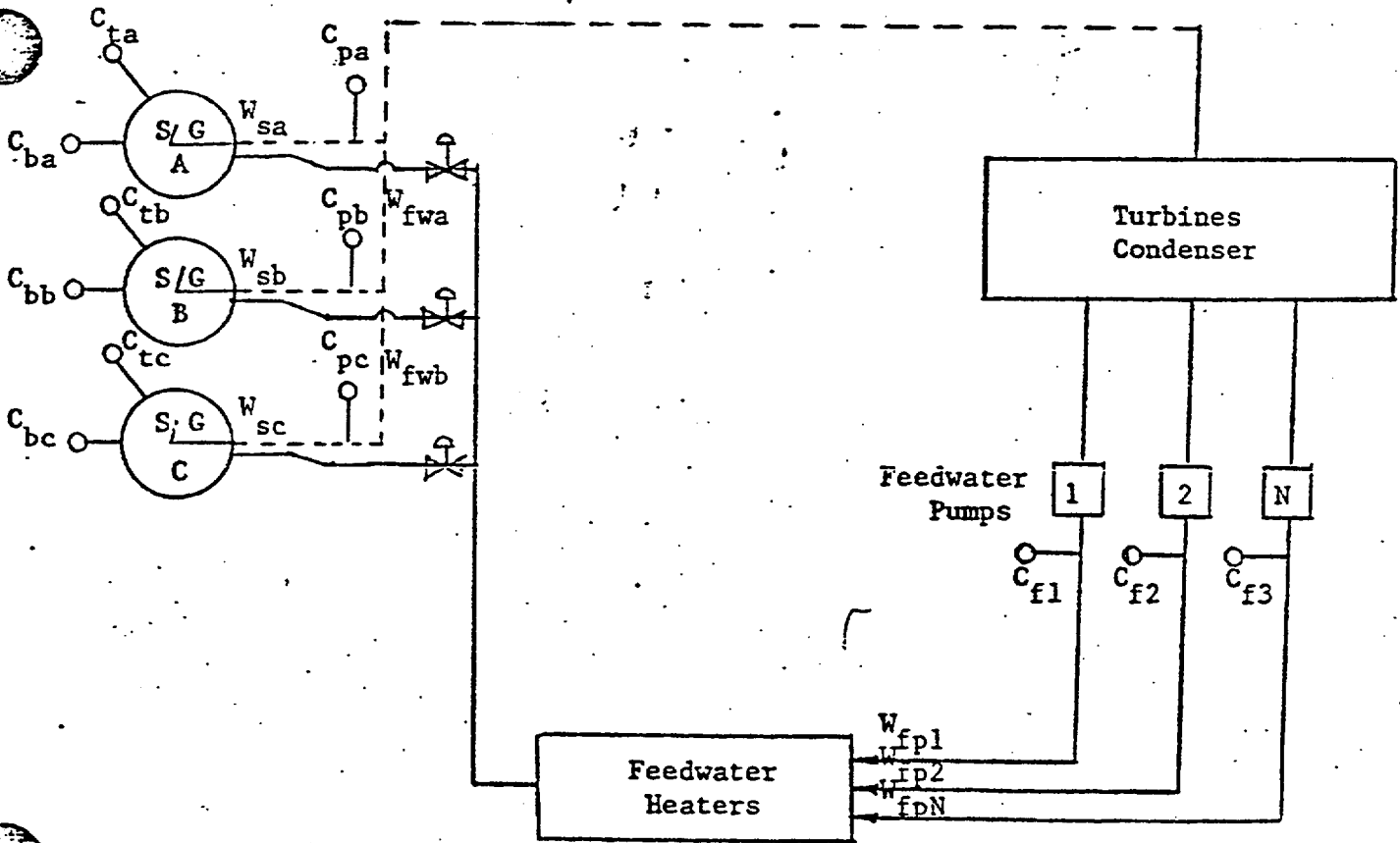
$$\sum N_{a_m} + = \sum N_{a_s} + \tag{1}$$

$$C_t(CO)(W_s) = C_s(W_s) \tag{2}$$

$$CO = \frac{C_s}{C_t} \tag{3}$$

Equation (3) is the general form for moisture carryover. For a three loop plant the important moisture carryover calculation is the average moisture carryover delivered to the turbine and is defined as:

$$\overline{CO} = 1/3 (CO_a + CO_b + CO_c) \tag{4}$$



$$\Sigma Na_s^+ = C_{sa} W_{sa} + C_{sb} W_{sb} + C_{sc} W_{sc} = \text{amount of sodium ion in steam}$$

$$\Sigma Na_w^+ = \sum_{n=1}^n C_{fn} W_{fn} = \text{amount of sodium ion in condensate}$$

$$\Sigma Na_s^+ = \Sigma Na_w^+$$

$$C_{sa} W_{sa} + C_{sb} W_{sb} + C_{sc} W_{sc} = \sum_{n=1}^n C_{fn} W_{fn} \quad (5)$$

$$\text{Let } C_{sa} = R_1 C_{sb} = R_2 C_{sc} \quad (5a)$$

$$C_{sa} W_{sa} + \frac{C_{sa} W_{sb}}{R_1} + \frac{C_{sa} W_{sc}}{R_2} = \sum_{n=1}^n C_{fn} W_{fn}$$

$$C_{sa} = \frac{\sum_{n=1}^n C_{fn} W_{fn}}{\left[ W_{sa} + \frac{W_{sb}}{R_1} + \frac{W_{sc}}{R_2} \right]} \quad (6)$$

From Equations (3) and (4)

$$\overline{CO} = \left[ \frac{100}{3} \right] \left[ \frac{C_{sa}}{C_{ta}} + \frac{C_{sb}}{C_{tb}} + \frac{C_{sc}}{C_{tc}} \right] \quad (7)$$

which becomes

$$\overline{CO} = \left[ \frac{100}{3} \right] (C_{sa}) \left[ \frac{1}{C_{ta}} + \frac{1}{R_1 C_{tb}} + \frac{1}{R_2 C_{tc}} \right] \quad (8)$$

Substituting Equation (6) into Equation (8)

$$\overline{CO} = \left[ \frac{100}{3} \right] \left[ \frac{\sum_{n=1}^n C_{fn} W_{fn}}{W_{sa} + \frac{W_{sb}}{R_1} + \frac{W_{sc}}{R_2}} \right] \left[ \frac{1}{C_{ta}} + \frac{1}{C_{tb} R_1} + \frac{1}{R_2 C_{tc}} \right] \quad (9)$$

During Equilibrium Conditions

$$W_{sa} = W_{fwa}$$

$$W_{sb} = W_{fwb}$$

$$W_{sc} = W_{fwc}$$

Substituting these values into Equation (9) the final form of the moisture carryover equation is derived if steam probes are available in each steam line.

$$\overline{CO} = \left[ \frac{100}{3} \right] \left[ \frac{\sum_{n=1}^n C_{fn} W_{fn}}{W_{fwa} + \frac{W_{fwb}}{R_1} + \frac{W_{fwc}}{R_2}} \right] \left[ \frac{1}{C_{ta}} + \frac{1}{R_1 C_{tb}} + \frac{1}{R_2 C_{tc}} \right] \quad (10)$$

If steam probes are not present it must be assumed that the carryovers from the steam generators are identical.

$$CO_a = CO_b = CO_c$$

Also:

$$CO = \frac{C_s}{C_t} \times 100$$

Therefore

$$C_{sa} = \frac{(CO)(C_{ta})}{(100)}$$

$$C_{sb} = \frac{(CO)(C_{tb})}{(100)}$$

$$C_{sc} = \frac{(CO)(C_{tc})}{(100)}$$

(11)

Substituting Equations 11 into Equation 5a

$$R_1 = \frac{C_{ta}}{C_{tb}}$$

$$R_2 = \frac{C_{ta}}{C_{tc}} \quad (12)$$

These R values are employed in Equation 10 if steam probes are unavailable.

For computational ease, define:

$$\text{Term 1} = W_{fwa} + \frac{W_{fwb}}{R_1} + \frac{W_{fwc}}{R_2} \quad (13)$$

$$\text{Term 2} = \frac{1}{C_{ta}} + \frac{1}{R_1 C_{tb}} + \frac{1}{R_2 C_{tc}} \quad (14)$$

Consequently Equation 18 becomes:

$$\overline{CO} = \left[ \frac{100}{3} \right] \left[ \begin{array}{c} n \\ \Sigma \\ n=1 \end{array} C_{fn} W_{fn} \right] \left[ \frac{\text{Term 2}}{\text{Term 1}} \right] \quad (15)$$

The circulation ratio can be determined by a mass balance of the sodium entering and leaving the tube bundle.

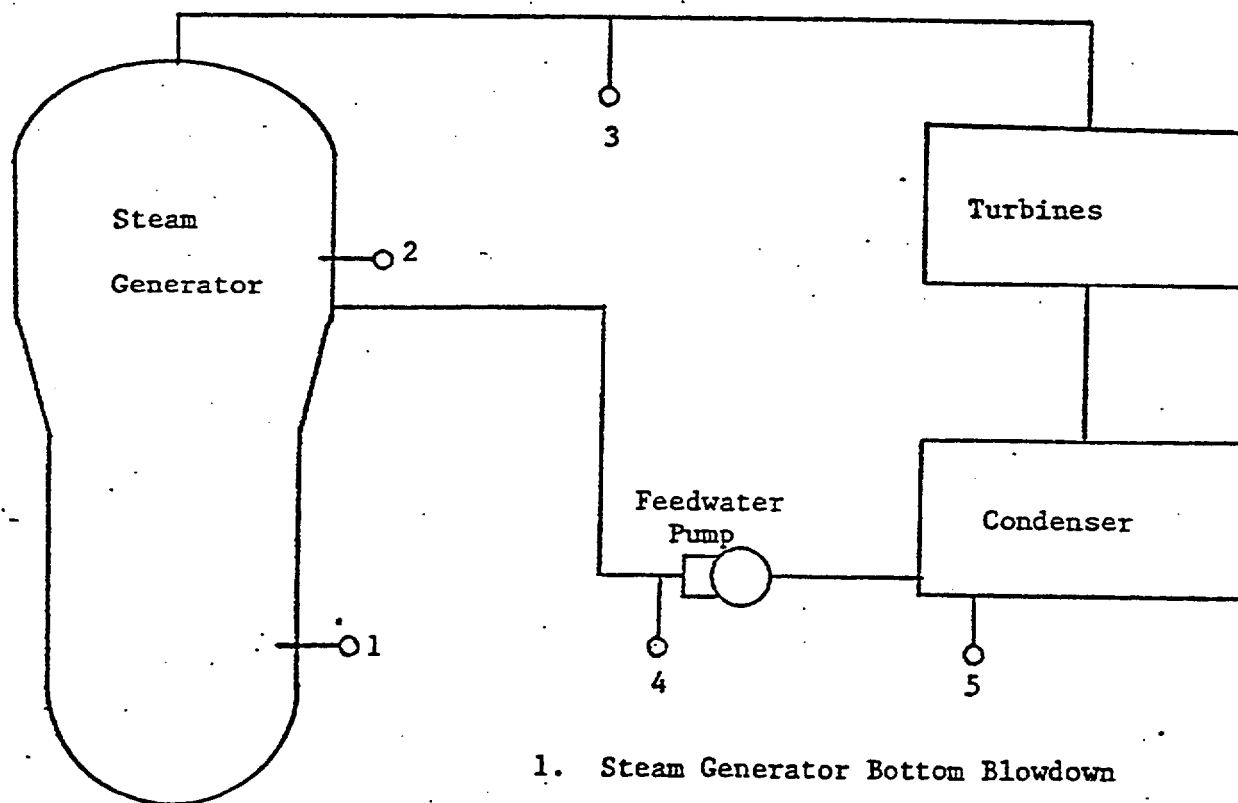
Amount of sodium entering tube bundle =  $\overline{C}_b (CR) (W_s)$

The boiling pressure reduces the water mass by  $W_s$ ,

so Amount of water leaving tube bundle =  $(CR-1)(W_s)$

and Amount of sodium leaving tube bundle =  $C_t (CR-1)(W_s)$

## 2.2 Sampling Points



1. Steam Generator Bottom Blowdown
2. Steam Drum Sampling Point
3. Steam Pipe Sampling Point
4. Feedwater Pump Discharge Sampling Point
5. Condenser Hotwell Sampling Point

$$\text{so } C_b(\text{CR})(W_s) = C_t(\text{CR}-1)(W_s)$$

$$\text{CR} = \frac{C_t}{C_t - C_b}$$

Since the reliability of the carryover equation rests on the accuracy of the steam and recirculating water samples, it is essential that the samples are representative. Sampling of the recirculating water presents little difficulty since the recirculating water is a homogeneous condensed flow. However, the acquisition of a representative steam sample is extremely difficult.

### 2.3 Circulating Water Sample

#### 2.3.1 Bottom Blowdown

A representative sample of the steam generator water can be obtained from the bottom blowdown. Due to the concentrating effects of circulation and boiling, this water sample does not represent the true sodium concentration of the moisture in the steam.

### 2.4 Recirculating Water Sample

#### 2.4.1 Steam Drum Sampling Tap

The steam drum sampling tap provides a sampling of the water separated from the steam in the separation equipment. This water sample represents the true sodium concentration of the moisture in the steam.

## 2.5 Steam Sample

### 2.5.1. Steam Probe

Although Tampa Division does not recognize sampling from a steam probe as being a valid or representative sample, if properly installed and utilized, it will indicate realistic trends but not realistic magnitudes. The steam probe must sample a two-phase flow and in doing so introduces a flow disturbance which can result in more water entering the nozzle than is representative.

Unless a very uniform mist flow exists in the steam pipe, it is improbable that a few holes in a cylindrical probe will extract a uniform sample. Even if a mist flow exists, the probe acts as a flow disturbance which appears to result in the flow entering the probe entraining greater moisture than the free stream as a result of the flow pattern around the probe. In addition, if the steam probe sample is to be realistic, then the sample must be extracted isokinetically. During isokinetic sampling, the velocity entering the probe ports is the same as the stream velocity in the pipe.

The sampling nozzle should be designed in accordance with Paragraph 8 of Reference 1 and installed in a straight run of pipe of a length equal to at least ten pipe diameters not located immediately after valves or bends. Additional installation instructions are given by Paragraph 10 of Reference 1.

### 2.5.2. Feedwater Pump Discharge Piping

The feedwater pump discharge pipe sampling point represents the total flow of the condensed steam. The sample is extracted through a pressure tap at an arbitrary rate. This point is recognized as the official steam sampling point since it represents the only total flow homogeneous liquid phase sample point present in the plant. Consequently, Tampa Division considers this as the most representative steam sampling point.

### 2.5.3. Condenser Hotwell

In lieu of the feedwater pump discharge piping sampling point, Tampa Division will recognize a condenser hotwell water sample. The condenser hotwell contains a homogeneous liquid phase but does not represent total flow since steam is extracted for feedwater heating and steam reheating. Separation between high and low pressure turbines also influences the validity of the sample. Consequently, the errors introduced by hotwell sampling can be significant.

## 3.0 Sampling Procedure

### 3.1 Water Chemistry

The water chemistry of the steam generator liquid shall be as normally specified for plant operation excepting the sodium level which shall be adjusted to 20 - 30 ppm by the addition of sodium phosphates in a molar ratio of 2.6 Na/PO<sub>4</sub> or less. Generally, the chemicals should be added to the feedwater downstream of the feed-



water control valve. Care must be taken to insure that all points of sodium addition to the secondary system do not fall between the steam generator outlet and any of the steam sampling points. Prior to testing, the steam generator should be operated at a constant load for a minimum of three hours following the addition of chemicals to attain chemical equilibrium in the circulating water as determined by sodium and/or phosphate analyses.

### 3.2 Preparation of Steam Generators

Prior to conducting a carry-over measurement, the steam generators should be operated at a low load (10 - 20%) for a period of approximately 24 hours with heavy, hourly blowdowns and phosphate additions to compensate for the phosphate lost as a result of the blowdowns. During this period, blowdown samples are to be taken periodically and checked for impurities such as oil, syndets, and suspended solids. The blowdowns are to be terminated with the absence of impurities and suspended solids concentration of 5 ppm or less.

Do not commence the carry-over test until it has been confirmed that the phosphates fed to the steam generators have come to equilibrium as determined by phosphate analysis.

### 3.3 Sampling Apparatus

The apparatus required for extracting the sample from the sampling point is described by Paragraphs 13 through 19 of Reference 1. In addition, the sample cooler must be leak free to insure reliable sampling.

### 3.4 Sampling Technique (Reference 2)

Considerable care must be exercised in obtaining the water samples since the samples are easily contaminated by atmospheric dust and other extraneous sources. To prevent touching the neck and reduce ambient contamination, an overflow bottle with a plastic shield should be employed. The 16 ounce polyethylene bottles must be rinsed free of any sodium, and the neck and the inside of the cap should not be touched.

Obtain the sample through rubber tubing attached to the effluent of the sample cooler and directed toward the overflow bottle. An inverted polyethylene funnel attached to the end of the tubing is intended to act as a contamination shield by resting on the neck of the overflow bottle. When ready to sample, merely lift the funnel from the overflow bottle to the neck of the sample bottle, taking care to avoid touching the ends of the tube or the bottle neck with your fingers. After filling the sample bottle, transfer the funnel back to the overflow bottle and immediately cap the sample bottle.

The sampling lines should be permitted to flow for at least one hour (or greater if required to obtain a flow that is visually clean) prior to sampling to flush the extraction system. Also, one hour of steady state operation should elapse prior to sampling following any load change.

### 3.5 Sampling Rates

The following sampling rates should be observed during testing.

1. Steam probe sampling shall be adjusted to give isokinetic sampling (i.e. the velocity entering the ports of the sample probe shall be the same as the velocity of the stream that is being sampled.)
2. Steam drum sampling rate is arbitrary and need only be adjusted to maintain a continuous rinsing of the sampling system.
3. Feedwater pump discharge sampling rate is arbitrary and need only be adjusted to maintain a continuous rinsing of the sampling system.
4. Condenser hotwell sampling rate is arbitrary and need only be adjusted to maintain a continuous rinsing of the sampling system.
5. Bottom blowdown sampling rate is arbitrary and need only be adjusted to maintain a continuous rinsing of the sampling system.

### 3.6 Sample Analysis

Obtain three representative samples from each sample point for each data point and analyze for sodium by means of flame emission spectroscopy. In addition to the samples collected for sodium analysis, collect a steam generator sample at each data point and analyze the sample for pH, conductivity, phosphate and chloride concentration.

### 3.7 Data to be Collected

The following data should be collected at the time that any set of samples is collected. It is recommended that data be taken at 30%, 70%, 90% and 100% load.

1. Feedwater flow rate of each steam generator
2. Feedwater temperature of each steam generator
3. Steam generator steam pressure of each steam generator
4. Steam generator water level of each steam generator
5. Flow rates and temperature in each sample pipe line of each steam generator
6. Date
7. Time
8. Electrical load
9. Three 16 ounce water samples each from the bottom blowdown, from each of the steam drum taps, and from each of the steam sampling points. (minimum recommended number samples = 36, 3 bottom blowdown from each steam generator, 3 steam probe samples from each steam generator, 3 samples from each feedwater pump discharge, and 3 steam drum samples from each generator).

### 3.8 Final Adjustment of Steam Generator Chemistry

At the conclusion of the carryover test, adjust the steam generator water chemistry back to the prescribed limits.

#### 4.0 Calculation Procedure

Moisture carryover determinations using steam sampling probes are considered unreliable because of the difficulties involved in obtaining a sample that is representative of the steam-water mixture flowing in the pipe. The carryover determined should be based on the feed-water pump discharge piping sample, but since this sample is unavailable it will be based on the condenser hotwell samples.

The moisture carryover is computed by employing the relations derived in Section II. The following page presents a calculation sheet which if completed will result in the moisture carryover being calculated according to accepted Tampa Division procedures.

3-LOOP MOISTURE CARRYOVER CALCULATION SHEET 1

Data

Calculated By \_\_\_\_\_

Date \_\_\_\_\_

Time \_\_\_\_\_

MWe \_\_\_\_\_

-----  
Steam Generator A

Feedwater Flow Rate 1 \_\_\_\_\_ ( $W_{fwa}$ )  
Feedwater Temperature 2 \_\_\_\_\_ ( $T_{fwa}$ )  
Steam Pressure 3 \_\_\_\_\_ ( $P_{sa}$ )  
Water Level 4 \_\_\_\_\_ ( $WL_a$ )

Steam Generator B

Feedwater Flow Rate 5 \_\_\_\_\_ ( $W_{fwb}$ )  
Feedwater Temperature 6 \_\_\_\_\_ ( $T_{fwb}$ )  
Steam Pressure 7 \_\_\_\_\_ ( $P_{sb}$ )  
Water Level 8 \_\_\_\_\_ ( $WL_b$ )

Steam Generator C

Feedwater Flow Rate 9 \_\_\_\_\_ ( $W_{fwc}$ )  
Feedwater Temperature 10 \_\_\_\_\_ ( $T_{fwc}$ )  
Steam Pressure 11 \_\_\_\_\_ ( $P_{sc}$ )  
Water Level 12 \_\_\_\_\_ ( $WL_c$ )

### 3-LOOP MOISTURE CARRYOVER CALCULATION SHEET 2

#### R Values Calculation Without Steam Probes

Date \_\_\_\_\_

Calculated By \_\_\_\_\_

Time \_\_\_\_\_

MWe \_\_\_\_\_

Water Level \_\_\_\_\_

Bottom Blowdown Sodium Concentration Steam Generator A      1 \_\_\_\_\_ (C<sub>ba</sub>)

Bottom Blowdown Sodium Concentration Steam Generator B      2 \_\_\_\_\_ (C<sub>bb</sub>)

Bottom Blowdown Sodium Concentration Steam Generator C      3 \_\_\_\_\_ (C<sub>bc</sub>)

Steam Drum Tap Sodium Concentration Steam Generator A      4 \_\_\_\_\_ (C<sub>ta</sub>)

Steam Drum Tap Sodium Concentration Steam Generator B      5 \_\_\_\_\_ (C<sub>tb</sub>)

Steam Drum Tap Sodium Concentration Steam Generator C      6 \_\_\_\_\_ (C<sub>tc</sub>)

Calculate R<sub>1</sub> Term:  $R_1 = \frac{C_{ta}}{C_{tb}}$       7 \_\_\_\_\_ (R<sub>1</sub>)

Calculate R<sub>2</sub> Term:  $R_2 = \frac{C_{ta}}{C_{tc}}$       8 \_\_\_\_\_ (R<sub>2</sub>)

### 3-LOOP MOISTURE CARRYOVER CALCULATION SHEET 3

#### Term 1 and Term 2 Calculation

Date \_\_\_\_\_

Calculated By \_\_\_\_\_

Time \_\_\_\_\_

MWe \_\_\_\_\_

Water Level \_\_\_\_\_

Feedwater Flow Rate Steam Generator A \_\_\_\_\_ (W<sub>fwa</sub>) 1

Feedwater Flow Rate Steam Generator B \_\_\_\_\_ (W<sub>fwb</sub>) 2

Feedwater Flow Rate Steam Generator C \_\_\_\_\_ (W<sub>fwc</sub>) 3

R<sub>1</sub> Term \_\_\_\_\_ (R<sub>1</sub>) 4

R<sub>2</sub> Term \_\_\_\_\_ (R<sub>2</sub>) 5

Steam Drum Tap Sodium Concentration Steam Generator A \_\_\_\_\_ (C<sub>ta</sub>) 6

Steam Drum Tap Sodium Concentration Steam Generator B \_\_\_\_\_ (C<sub>tb</sub>) 7

Steam Drum Tap Sodium Concentration Steam Generator C \_\_\_\_\_ (C<sub>tc</sub>) 8

Bottom Blowdown Sodium Concentration Steam Generator A \_\_\_\_\_ (C<sub>ba</sub>) 9

Bottom Blowdown Sodium Concentration Steam Generator B \_\_\_\_\_ (C<sub>bb</sub>) 10

Bottom Blowdown Sodium Concentration Steam Generator C \_\_\_\_\_ (C<sub>bc</sub>) 11

Calculate Term 1

$$\text{Term 1} = W_{fwa} + \frac{W_{fwb}}{R_1} + \frac{W_{fwc}}{R_2} \quad 12 \text{ _____ (Term 1)}$$

Calculate Term 2

$$\text{Term 2} = \frac{1}{C_{ta}} + \frac{1}{R_1 C_{tb}} + \frac{1}{R_2 C_{tc}} \quad 13 \text{ _____ (Term 2)}$$



3-LOOP MOISTURE CARRYOVER CALCULATION SHEET 4

Plant Average Moisture Carryover Calculation

Date \_\_\_\_\_

Calculated By \_\_\_\_\_

Time \_\_\_\_\_

MWe \_\_\_\_\_

Water Level \_\_\_\_\_

Sodium Concentration Feedwater Pump 1 Discharge Sample \_\_\_\_\_ ( $C_{f1}$ ) 1

Sodium Concentration Feedwater Pump 1 Discharge Sample  
at 30% Load \_\_\_\_\_ ( $C_{f1c}$ ) 2

Sodium Concentration Feedwater Pump 2 Discharge Sample \_\_\_\_\_ ( $C_{f2}$ ) 3

Sodium Concentration Feedwater Pump 2 Discharge Sample  
at 30% Load \_\_\_\_\_ ( $C_{f2c}$ ) 4

Sodium Concentration Feedwater Pump 3 Discharge Sample \_\_\_\_\_ ( $C_{f3}$ ) 5

Sodium Concentration Feedwater Pump 3 Discharge Sample  
at 30% Load \_\_\_\_\_ ( $C_{f3c}$ ) 6

NOTE: Insert zero for all values relating to pumps  
that do not exist.

Feedwater Pump 1 Flow Rate \_\_\_\_\_ ( $W_{f1}$ ) 7

Feedwater Pump 2 Flow Rate \_\_\_\_\_ ( $W_{f2}$ ) 8

Feedwater Pump 3 Flow Rate \_\_\_\_\_ ( $W_{f3}$ ) 9

Calculate  $\sum_{n=1}^n (C_{fn} - C_{fnc}) W_{fn}$

$= (C_{f1} - C_{f1c}) W_{f1} + (C_{f2} - C_{f2c}) W_{f2} + (C_{f3} - C_{f3c}) W_{f3}$

10  $\sum_{n=1}^n (C_{fn} W_{fn})$

Insert Term 1

11 \_\_\_\_\_ (Term 1)

Insert Term 2

12 \_\_\_\_\_ (Term 2)

Calculate Plant Average Moisture Carryover

$$\overline{CO} = \left[ \frac{100}{3} \right] \left[ \sum_{n=1}^n (C_{fn} W_{fn}) \right] \left[ \frac{\text{TERM 2}}{\text{TERM 1}} \right] = \text{_____} = \overline{CO}$$

## 5.0 References

1. ASME Power Test Codes, Part 11, "Quality and Purity of Steam", PTC 19.11 - 1970.
2. "Method of Sampling for Sodium Determination", Betz Technical Data Sheet, Betz Laboratories, Inc., Philadelphia, Pa.
3. Sokolowski, Peter F., "General Procedure for Determining Moisture Carryover Performance of Steam Generators in a Pressurized Water Nuclear Plant", Rev. 2, August 20, 1969, Westinghouse Electric Corporation, Lester, Pa.
4. Bennett, Robert R., "General Procedure for Determining the Moisture Carryover Performance of the Steam Generators in a 3 Loop Pressurized Water Nuclear Plant", WTD-PWEE-71-3, February, 1971, Westinghouse Electric Corporation, Tampa, Florida.

QUESTION 1.17

In Figures 5.3.2-4 and 5.3.2-5 the values for pressure given under "Data Ranges" and "Legend" do not correspond. The inlet quality range does not correspond to the curves on the figures. Please correct these inconsistencies. The curves in Figure 5.3.2-4 indicate that swirl vane efficiency increases with flow rate while Figure 5.3.2-5 indicates that the efficiency decreases with flow rate. Discuss the reasons for this inconsistency. Provide the actual data points for each curve and discuss the test procedure by which the data was obtained.

Answer 1.17

There are no inconsistencies between the "Data Ranges" and the "Legend" on either Figure 5.3.2-4 or 5.3.2-5. The information supplied under the heading "Data Ranges" specifies the range of thermodynamic variables over which data was taken to arrive at the empirical correlation depicted by the graph. The "Legend" simply identifies the parametric values of pressure which were chosen for plotting.

There also is no inconsistency in the trend indicated in Figures 5.3.2-4 and 5.3.2-5. It must be noted that different separator devices are being addressed in each graph. Because of the different design of the two devices, the trends exhibited by each should not be expected to be the same.

As discussed in the response to question 1.15, the graphs are parametric plots of an empirical, steady-state test of separator performance. The data is also presented in that response.

QUESTION 1.18

Page 8-3 and 8-4 indicate there are seven types of flow paths plus two special flow paths which are calculated by subroutine SCONN. Provide a complete description of the calculations made for special flow paths in subroutine SCONN and discuss their usage in steam generator analysis.

Answer 1.18

The seven standard flow links used in the TRANFLO code are:

1. Regular connector -

Regardless of flow direction, this type of flow path is assumed to be composed of single-phase or two-phase flow as determined by using the Armand correlation and the thermodynamic conditions in the source node. Flow rate is determined by the momentum equation described in Section 3 of the WCAP and the energy transported by the flow is determined by the flow quality.

2. Saturated steam flow only -

Same as a regular connector except that the flow quality is always 1. If the source node is either subcooled or superheated, the flow type reverts to a regular connector and the flow is subcooled water or superheated steam as is appropriate.

3. Saturated liquid flow only -

Same as saturated steam only connector except the flow composition is saturated liquid rather than saturated steam.

4. Steam flow in positive flow direction and water flow in negative flow direction -

Combination of the preceding two flow types with flow direction controlling type selection.

5. Steam flow in positive flow direction and regular flow in negative flow direction -

Combination of flow types 1 and 2 above with type selection determined by flow direction.

6. Water flow in positive direction regular flow in negative direction -

Combination of flow types 1 and 3 above with type selection determined by flow direction.

7. Cross flow through a tube bundle -

Regular flow path which uses a crossflow friction factor for a regular spaced tube bundle to determine the friction pressure loss in the momentum equation (see response to Question 1.5).

Generally, when modeling steam generators, only two of the above connector types would be used. Those are the type 1 regular connectors and the type 7 crossflow connectors. The crossflow types are used in the U-bend region of the tube bundle and in the preheater crossflow passages in the Model D steam generator.

The subroutine SCONN is used only to define the characteristics of the separator models that are discussed in Section 4.3 of WCAP-8821. These connectors are the swirl vanes, the chevrons, the swirl vane drains, and the chevron drains. The manner in which these flow links are modeled in SCONN is also explained in Section 4.3. The sign option on XFT = +4 as shown on Page 8-4 was originally provided to allow the user greater flexibility in specifying which thermodynamic variables of a flow are to be established in SCONN (i.e. the separator related flow paths). This option is not used and currently values of quality, void fraction, and specific enthalpy are each specified in SCONN.

In the case of the drain paths, an elevation correction is also made. In the swirl vanes, this correction is the centrifugal term (see response to Question 1.12). The correction to the chevron drain head is based on the amount of water which resides in the drains (see Page 4.24 of WCAP-8821).

QUESTION 1.19

Section 5.2 describes an analysis of a steamline break using the SATAN VI code. Provide a comparison of significant assumptions made by the SATAN VI code and the TRANFLO code. Include comparisons of two-phase pressure losses, slip velocity and primary-to-secondary heat transfer. Discuss the differences in assumptions for the parallel flow paths illustrated in Figure 5.2-1 (i.e., paths 15-A and 15-B).



Answer 1.19

The SATAN model used to produce the results presented in Section 5.2 was identical in noding scheme to that of the TRANFLO model. The primary heat were also set up to duplicate the scheme in TRANFLO. However, the codes do differ in some methods of calculations.

The relative phase velocities or phase slip is taken into account by the use of the modified Armand correlation in the flow connectors of the TRANFLO code while the SATAN code uses the Zuber drift flux model. The drift flux model is completely discussed in Section 2.2.2 of WCAP-8302.

The major differences between these two models are as follows:

1. The drift flux model is a non-homogeneous model while the Armand correlation is homogeneous.
2. In regions where velocities are low in a vertical flow path, the drift flux model allows counter-current flow to occur. This is not possible with Armand.
3. The prediction of the entrainment threshold is inherent in the drift flux model while a separate correlation (the Davis correlation) must be used in conjunction with Armand.
4. The drift flux model is only used in flow paths with elevation change. Satan models the rest of the paths as homogenous without slip. TRANFLO assumes slip in all two phase flow paths.

The pressure drop calculations are done using different methods in the two codes. The TRANFLO method is to calculate the pressure drop using the well known Darcy formula and adjust the value of pressure drop by calculating an effective specific volume based on flowing quality from the Armand void correlation as shown in Section 3 of WCAP-8821 (See response to Question 1.1). The SATAN method is to calculate a two phase multiplier as illustrated in Appendix C of WCAP-8302 using the HTFS two phase pressure drop correlation. The quality used

in this correlation is also flowing quality from the modified Armand correlation. Table 1 shows a comparison of predicted delta P calculated by each code for 100 feet of a 1 inch pipe at various flowrates.

The two codes handle primary to secondary heat transfer in essentially the same way. Table 2 summarizes the heat transfer correlation used in the two codes. Note that all correlations are the same with the exception of that for forced convection to superheated steam. SATAN uses the McEligot correlation. This difference, however, should have a negligible effect on the results since this condition would not be expected to exist during the first eight seconds of transient for which the comparison in WCAP-8821 is presented.

The flow paths 15-A and 15-B in Figure 5.2-1 of WCAP-8821 use no different assumptions. They merely represent two separate flow paths from node 15 to node 16. Path 15-A represents the flow through node 15 and then up through the five windows in the baffle plate which open to node 16. Path 15-B represents the leakage flow path from node 15 to node 16 through the tube holes (leakage around the tubes).

TABLE 1

SATAN/TRANFLO  $\Delta P$  COMPARISON

<u>QUALITY</u> (%)	<u>PRESSURE DROP</u> (PSI)			
	SATAN		TRANFLO	
	<u>1 lb/sec</u>	<u>2 lb/sec</u>	<u>1 lb/sec</u>	<u>2 lb/sec</u>
0	.1	.5	.1	.4
10	.9	3.1	.4	1.5
20	1.4	5.1	.9	2.8
30	1.9	6.6	1.2	4.1
40	2.3	7.9	1.6	5.4
50	2.6	8.9	2.0	6.7
60	2.7	9.5	2.3	7.7
70	2.8	9.9	2.3	7.9
80	2.8	9.9	2.1	7.1
90	2.7	9.5	2.6	8.8
100	2.4	8.7	3.1	10.5

TABLE 2  
COMPARISON OF HEAT TRANSFER CORRELATIONS

<u>FLUID CONDITIONS</u>	<u>TRANFLO</u>	<u>SATAN</u>
Subcooled Forced Convection	Dittus Boelter	Dittus Boelter
Forced Convection to Superheated Steam	Heineman	McEligot*
Nucleate Boiling	Thom	Thom
Transition Boiling	Westinghouse Transition Boiling Correlation	Westinghouse Transition Boiling Correlation
Film Boiling	Dougall & Rohsenow	Dougall & Rohsenow
Subcooled Film Boiling	Sandberg, Bishop & Tong	Sandberg, Bishop & Tong

-----  
 \*See page 2-88 of WCAP-8302

## QUESTION 2.1

On page 1-2 it is stated that the break quality versus time data generated by the TRANFLO code is input to the MARVEL code which is then used to generate mass and energy release data for containment analysis. It is further stated that the initial fluid mass in the steam generator is minimized in the TRANFLO analyses and maximized in the MARVEL analyses. Use of quality versus time data from the TRANFLO code would appear to cause the mass of entrained liquid released by the MARVEL code to be greater than that predicted by the TRANFLO code. For each break analyzed provide a comparison of the entrained liquid mass predicted by the TRANFLO code to that calculated by the MARVEL code.

Answer 2.1

The amount of entrained liquid calculated by the MARVEL code is, in fact, less than the amount predicted by the TRANFLO code. This is due to increasing the flow quality versus time data from TRANFLO by 0.1 before inputting it to the MARVEL code (see Section 3.2.2 of WCAP-8822). This effect is demonstrated in the following approximates of the integral water relief during blowdown from each code:

Total Entrained Water (lb)

	<u>TRANFLO</u>	<u>MARVEL</u>	
I. 102% Power	[	]	
1.4 ft <sup>2</sup> , DER			(a,c)
0.7 ft <sup>2</sup> , DER			
II. 70% Power			
1.4 ft <sup>2</sup> , DER			
0.6 ft <sup>2</sup> , DER			
III. 30% Power			
1.4 ft <sup>2</sup> , DER			
0.5 ft <sup>2</sup> , DER			
IV. 0% Power			
1.4 ft <sup>2</sup> , DER			
0.2 ft <sup>2</sup> , DER			

QUESTION 2.2

The version of the MARVEL code (WCAP-7635) which you reference has not been submitted to the NRC. Some of the calculations to which you refer in WCAP-8822 are not present in the version of MARVEL that we are reviewing. Please provide this document.

Answer 2.2

The updated MARVEL report has been submitted for review as WCAP-8843.



QUESTION 2.3

Provide the calculational model used to calculate heat transfer from the primary metal to the primary fluid that is discussed on page 3-6.

Answer 2.3

See section 2-34 of WCAP-8843.

#### QUESTION 2.4

Provide and justify the heat transfer coefficients used in the MARVEL code to calculate heat flow from the steam generator tubes to the steam generator fluid for the regions above and below the two-phase level. When the two-phase level drops sufficiently to uncover the steam generator tubes, additional heat transfer to the steam will produce superheating. Discuss how this effect is considered in the MARVEL code.

#### Answer 2.4

Heat transfer to steam is not included in the MARVEL steam generator model. An input variable specifying the effective tube height is used in MARVEL and the calculated water level is compared to this input height to determine if the tubes are uncovered during a transient. Water level is determined based on the bulk quality of the steam generator secondary fluid, the steam generator secondary volume, and input tables of steam generator water volume versus height above the tube sheet. A more detailed explanation of the water level calculations can be found in Section 2-18 of WCAP-8843. When the calculated water level drops below the input value of tube height, heat transfer area is reduced by the ratio of water level to effective tube height. No heat transfer is assumed to occur above the calculated water level. Heat transfer is determined using the Jens-Lottes heat transfer correlation.

### QUESTION 2.5

The heat transfer coefficient from the steam generator tubes to steam generator liquid is modified by a multiplier proportional to the two-phase level within the tubes. Describe how the two-phase level is calculated in the MARVEL code. Provide justification for this model. For the 0.6 ft<sup>2</sup> break at full power, provide a comparison of the two-phase level as a function of time predicted by the MARVEL code with that predicted by the TRANFLO code. Provide the mass and energy release to the containment for the above break using the MARVEL code and the two-phase level predicted by the TRANFLO code.

Answer 2.5

The MARVEL calculation of steam generator water level uses an input table of steam generator secondary side volume versus height above the tube sheet. At each time step in a transient calculation the quality determined from the energy balance and the total mass determined from the mass balance are used to find the amount of liquid and the amount of vapor in the steam generator shell. The volume of liquid is then found using the saturation density. This volume is compared to the volume versus height for the steam generator to give a water level (See response to Question 2.4).

Loss of heat transfer due to decreasing water level depends upon the calculated water level and another input variable which specifies the "effective tube height" of the steam generator. This variable is used as follows:

1. If calculated water level  $>$  "effective tube" height

then 
$$UA_{trans} = UA_{nom} \times K$$

where  $K$  = correction to account for changes in the primary and secondary heat transfer coefficients due to changes in flow, pressure and temperature.

2. If calculated water level  $<$  "effective tube" height

then 
$$UA_{trans} = UA_{nom} \times K \times \frac{\text{calc. water level}}{\text{effective tube height}}$$

Thus, this calculation effectively reduces the heat transfer area in the bundle linearly with decreasing water level once the calculated level drops below the input value for effective tube height.

Obviously the model is not accurate unless a proper value of effective tube height is chosen. Also, this model would not be expected to be adequate to define heat transfer in the steam generator during periods of rapid depressurization accompanied by high void generation rates and possible tube dryout or DNB as might be expected to occur in the first 15 - 30 seconds following a break. However, it has been shown (Ref. 3) that during quasi-stable pressure/flow conditions in the steam generator, a linear decay in heat transfer capability with decreasing water level is an adequate model.

Considering these facts, the MARVEL heat transfer modeling, as used in the generation of steam line break mass/energy releases, is considered to be adequate for several reasons. First, during the early part of the blowdown described in WCAP-8822, the MARVEL model assumes the bulk UA in the steam generator is equal to the nominal value corrected only for the effects of pressure, temperature and flow changes. Thus no credit is taken for possible loss of heat transfer as a result of high voiding and possible dry-out or DNB in the steam generator tubes during the initial depressurization following the break. Also, in the analyses presented in WCAP-8822, loss of heat transfer resulting from inventory loss occurs only after long delays in the MARVEL calculation. At this time the depressurization rate and steam flow rates are very low (see the attached table), and the use of a model such as that in MARVEL should be adequate for this portion of the blowdown.

The remaining consideration is the value used for tube height. In the MARVEL calculations, an effective tube height of approximately 27 feet was used since this is the actual tube height in Model D steam generators. However, sensitivity studies were performed to determine the effect of using smaller values of tube height. A comparison between the results of a 1.4 ft<sup>2</sup> break at 102% power using a tube height of 1' showed the following differences in break flow, steam pressure, and heat transfer after 200 seconds:

<u>Variable</u>	<u>Magnitude of Difference</u>
Break Flow	< 15 lb/sec
Steam Pressure	< 15 psi
Heat Transfer	< 2.5% nominal heat transfer

Following 200 seconds, these values begin to diverge due to uncovering of the tubes in the reference case. However, as pointed out on Page 3-11 of WCAP-8822, the difference in total energy release for these two cases differ by only 2.8% after 300 seconds.

Finally, we cannot respond to your request for the two phase level versus time from the TRANFLO code. As explained in WCAP-8821, the TRANFLO code uses homogeneous modeling in all fluid nodes. Therefore, it does not predict a water level in the steam generator.



STEAM GENERATOR CONDITIONS AT TIME REDUCTION IN  
UA BEGINS AS A RESULT OF WATER LEVEL REDUCTION

<u>Break</u>	<u>Time UA Reduction*</u> <u>Begins (sec)</u>	<u>Steam Flow</u> <u>(lb/sec)</u>	<u>Steam Pressure</u> <u>Decay Rate (psi/sec)</u>	<u>Power Level</u> <u>(%)</u>
1.4 ft <sup>2</sup> DER	90	769	0.9	102
1.4 ft <sup>2</sup> DER	55	833	2.1	70
1.4 ft <sup>2</sup> DER	78	680	1.1	30
1.4 ft <sup>2</sup> DER	110	544	0.7	0
0.7 ft <sup>2</sup> DER	130	587	0.9	102
0.6 ft <sup>2</sup> DER	160	524	0.7	102
0.6 ft <sup>2</sup> DER	225	439	0.5	70
0.5 ft <sup>2</sup> DER	> 300	< 372	< 0.5	70
0.5 ft <sup>2</sup> DER	> 300	< 310	< 0.5	30
0.4 ft <sup>2</sup> DER	> 300	< 282	< 0.5	30
0.2 ft <sup>2</sup> DER	> 300	< 112	< 0.7	0
0.1 ft <sup>2</sup> DER	> 300	< 68	< 0.7	0

\* Time when  $\frac{\text{water level}}{\text{effective tube height}} = 0.99$

QUESTION 2.6

Page 3-14 states that auxiliary feedwater flow is set equal to 20% of normal loop flow. Discuss the conservatism of this value for containment analysis.

## Answer 2.6

The value of 20% of nominal loop flow ( $\sim 1500$  gpm) was selected as a reasonable upper bound on the maximum auxiliary feed flow which would be supplied to one steam generator following a steam line break. This assumption is in accordance with current design recommendations to Westinghouse customers which specify that auxiliary feed system designs should limit the maximum flow to a depressurized steam generator to rates in the range of 1100 - 1400 gpm. This recommendation is made specifically to limit the energy release to containment following a steam line break.

However, the assumption of 1500 gpm auxiliary feed flow in the analysis described in WCAP-8822 has little effect on the blowdown releases provided in Appendix A of that WCAP. As discussed in Section 3.1.5, the effects of feedwater addition on blowdown flow is small, particularly in the long term. Thus the assumption of a larger or a smaller flow would not significantly change the blowdown data presented in Appendix A. If the blowdown flow is not changed, the only remaining parameter of importance is the total mass added to the steam generator. For conservatism, this mass should be large since all the water added by the auxiliary feedwater system will exit the broken steam line as steam. To insure that this mass is maximized, the maximum plant auxiliary feed flow is used in the dryout calculations described in paragraphs III.1.D and III.4.D.4 of the appendix. Additionally, when considering the full double-ended ruptures, the maximum auxiliary feedwater flow for the plant is also assumed to be the minimum value for the blowdown rate in the long term (see paragraph III.3 of Appendix A). Both of these calculational assumptions coupled with the minimal effect of feed water on blowdown flows assure that the total releases, as determined using Appendix A, are conservative with respect to auxiliary feed flow.

QUESTION 2.7

Provide and justify the feedwater flashing model in the MARVEL code discussed on page 3-14.

Answer 2.7

The MARVEL feedline flashing model is described in WCAP-8843, Section 2-23.

### QUESTION 2.8

On page 3-12 the low steamline pressure setpoint is said to be 600 psia for isolation of the steamlines for the 0.6 ft<sup>2</sup> break at full power. Figure 4-3 and Table IV-3 indicate that a steam pressure of 600 psia is reached in about 50 seconds following rupture. Table IV-3 indicates that the steamlines are isolated at 15 seconds following rupture. Discuss this apparent inconsistency and provide a detailed discussion of the sequence of events which lead to a main steamline isolation.

Answer 2.8

A discussion of the Westinghouse steam line isolation protective system is provided on Page 2-14 through 2-18 of WCAP-8822. In this discussion it is pointed out that the steam pressure signal used in the isolation logic is lead/lag compensated. The lead/lag compensation is included specifically for the purpose of anticipating low steam pressure conditions based on the rate of change of steam pressure. As an indication of the effectiveness of this circuitry, the following table shows the time for the compensated pressure to decrease 400 psi from its initial value given different linear decay rates of the actual steam pressure. It is this lead/lag compensation which causes the apparent inconsistency between the steam pressure and the isolation time given in Table IV-3. In summary, there is no inconsistency.

Effects of Lead/Lag Compensation  
on Measured Steam Pressure

<u>Pressure Decay</u> <u>Rate (psi/sec)</u>	<u>Time for Actual</u> <u>Pressure to Drop 400 psia</u>	<u>Time for Signal</u> <u>to Drop 400 psia</u>
-1	400	355 sec
-2	200	155
-5	80	35
-10	40	6.73
-15	26.67	3.59
-20	20	2.47
-25	16	1.88
-50	8	0.86

It is important to note, also, that Table IV-3 does not indicate that the steam lines are isolated in 15 seconds. As discussed in paragraph III.1A of Appendix A of WCAP-8822, and as indicated in the sample calculations in that appendix, and as pointed out by the footnote to

Table IV-3, isolation results after sufficient time has passed for an isolation signal to be generated, for the instruments to respond, for the signal to be processed, and for the isolation valves to close. The 15 seconds indicated in the reverse flow portion of Table IV-3 is not related to this isolation time, but is an arbitrary time duration which was judged to be sufficiently long to provide adequate data for all cases to be analyzed. In general, only a portion of the table is used to specify reverse flow.

The sequence of events which will result in steamline isolation on a Westinghouse designed plant is as follows: When the appropriate conditions in the plant are sensed by the safety grade instrumentation of the reactor protection system, a signal is generated and transmitted through redundant circuitry to the main steam stop valves requiring them to close. The main steam stop valves are fast acting air operated valves which, in case of failure, would fail closed.



### QUESTION 2.9

Provide analyses of a spectrum of split type ruptures at various power levels. These break types may produce mass and energy release rates to the containment greater than the double-ended ruptures analyzed in WCAP-8822. For example, for a four-loop plant, a split type rupture of  $2.4 \text{ ft}^2$  at full power would have the same effective area per steam generator as the 0.6 square foot break which you have analyzed with no entrainment. Following isolation of the steamlines, the effective area for one steam generator would be  $1.4 \text{ ft}^2$  which is the area of the flow restrictor. At this time, the mass of water in the ruptured steam generator would be less than for the  $1.4 \text{ ft}^2$  double-ended rupture which you have analyzed and the amount of entrainment would be reduced. The analysis of only double-ended ruptures, therefore, does not appear to be conservative for containment analysis.

## Answer 2.9

It is our position that the full double ended rupture blowdowns provide a bounding case for the type of split rupture postulated in Question 2.9. A justification (using the full power cases as an example) of this judgement follows.

1. For a  $0.6 \text{ ft}^2/\text{loop}$  rupture, the maximum time to generate a steam line isolation signal is no greater than 4.5 seconds, and will only be delayed this long if there is no increase in feedwater flow following the rupture. A best estimate calculation of the delay until isolation indicates times on the order of 1.0 to 1.3 seconds. Allowing five seconds for closure of the steam line isolation valve, a  $2.4 \text{ ft}^2$  split break in a 4 loop plant will look like a  $1.4 \text{ ft}^2$  double-ended rupture to one steam generator after a delay of only about 6 seconds. The attached figure demonstrates that this postulated 6 second delay has very little effect on the calculated entrainment in the blowdown.

Three curves are shown on the figure. Curve 1 is the entrainment transient for a  $1.4 \text{ ft}^2$  DER starting at time = 0. Curve 2 represents  $0.6 \text{ ft}^2/\text{loop}$  split rupture with steam line isolation occurring at 6 seconds. (This curve is plotted with the time scale shifted by 6 seconds to show a direct comparison with the first curve). As the figure shows, there are only small differences between the entrainment history for the  $1.4 \text{ ft}^2$  DER and the entrainment history for a  $1.4 \text{ ft}^2$  break which is preceded by 6 seconds of depressurization through an effective break area of  $0.6 \text{ ft}^2$ . The final curve on the Figure shows the entrainment history which was used in the actual calculation of release mass and energy for the  $1.4 \text{ ft}^2$  DER with the MARVEL code. As explained in Section 3.2.2 of WCAP-8822, this entrainment transient is equivalent to curve 1 plus 0.1, and, as the figure shows, bounds both curves 1 and 2.

2. Another factor which contributes to the judgement that the  $1.4 \text{ ft}^2$  DER is bounding is consideration of the additional inventory added to the containment from the intact steam generator loops. For the  $0.6 \text{ ft}^2/\text{loop}$  split, the energy from the intact units prior to an isolation at 6 seconds is equal to approximately 25 MBtu for a four loop plant. Following a  $1.4 \text{ ft}^2$  DER, the energy added from the intact units is approximately 60 MBtu. Even if the maximum delay time to isolation is assumed for the smaller break, the energy from the intact loops due to the additional 4.5 seconds of blowdown totals only about 41 MBtu; still significantly less than the energy added in the large break situation.
3. The effects of the blowdown from the steam piping should also be less severe for the  $0.6 \text{ ft}^2/\text{loop}$  split rupture. The total piping inventory for both this break and the large break should be essentially the same; however, the rate at which the energy is added to containment is lower for the smaller break.
4. The amount of mass added to the faulted steam generator from the main feedwater system would also be expected to be higher for the large double-ended rupture. This can be seen by comparing the depressurization rate for the two breaks given in Section IV of WCAP-8822. The DER causes a much larger pressure decay in the first 10 seconds of blowdown than does the  $0.6 \text{ ft}^2$  break. Generally this would result in greater feed flows to the steam generator prior to feed isolation, and thus greater total energy release from the full DER. However, even if very conservative assumptions are made, viz. feed flow to the faulted steam generator equal to 200% of nominal for either break and time to isolation for the smaller break 5 seconds longer than for the large break, the energy released by the small break blowdown is only on the order of 12 - 13 MBtu more than is released by the large break. This amount of energy is not sufficient to compensate for the additional energy added due to the blowdown from the intact steam generator units during a large break (see (2) above).

Similar arguments may be made for each of the power levels investigated in WCAP-8822. Thus, it is our position that an evaluation of the 1.4 ft<sup>2</sup> double-ended steam line rupture provides a bounding analysis for the largest split rupture without moisture entrainment.

COMPARISON OF THE ENTRAINED WATER FROM A  
1.4ft<sup>2</sup> DER AND A 0.6ft<sup>2</sup>/LOOP SPLIT

---

Effluent Quality

(a,c)

QUESTION 2.10

Provide analyses for steamline breaks within containment assuming loss of offsite power and loss of one diesel generator.

## Answer 2.10

The assumption of the loss of offsite power at the time of a steam line rupture and the simultaneous failure of one diesel generator would have two effects on a mass/energy release calculation. First would be the reduction and possible delay of safety injection flow due to loss of the one diesel and starting delays of the operational diesels. The second effect would be the loss of the forced reactor coolant flow due to the loss of ac power to the coolant pumps.

The effects of the loss of a safety injection pump train has already been included in the analysis presented in WCAP-8822 via use of a safety injection flow curve typical of minimum safeguards capability (see Figure 3.1.4-1, WCAP-8822). Delays to account for diesel starting were not included in the analyses since it is believed that the effects of tripping the reactor coolant pumps is of much greater benefit in reducing blowdown releases than is the penalty of an additional 5 - 10 seconds delay in the initiation of safeguards flow. There are several justifications for this position, one of which is provided in Section 3.1.7 of WCAP-8822.

A better indication of the total effect of loss of offsite power and loss of one diesel generator can be found in section 15.4.2 of RESAR-3S. The analysis described there considers steam line rupture both with and without offsite power available and uses minimum safety injection flows and appropriate delays for diesel starting. Inspection of Figures 15.4-20 and 15.4-21 in RESAR-3S indicate the validity of the conclusion of Section 3.1.7 of WCAP-8822, i.e. for mass/energy release determinations the blowdown release rates are higher when ac power is available, and, because the core cooldown is more severe with the reactor coolant pumps running, the power generation in the core is greater with offsite power available.

The only remaining consideration is the effect of the reduced blowdown flow rate on entrained liquid. It might be expected that the reduced

flow would result in less water entrainment. This in fact is the case as is shown in the attached graph which shows the entrainment in the blowdown from a 1.4 ft<sup>2</sup> double-ended rupture at full power both with and without the reactor coolant pumps running. The effect on the entrained water is small, however, and in either case is bounded by the entrainment history (also shown on the attached graph) which was used in the calculations described in WCAP-8822.

As a result, it is our judgement that the blowdown releases provided by Safety Analysis Standard 12.2, Rev. 1 (Appendix A of WCAP-8822) bound the mass/energy releases which would result from analyses which consider the effects of both loss of ac power and loss of one diesel generator.



EFFECTS OF RCP TRIP ON ENTRAINMENT

Effluent Quality

(a,c)

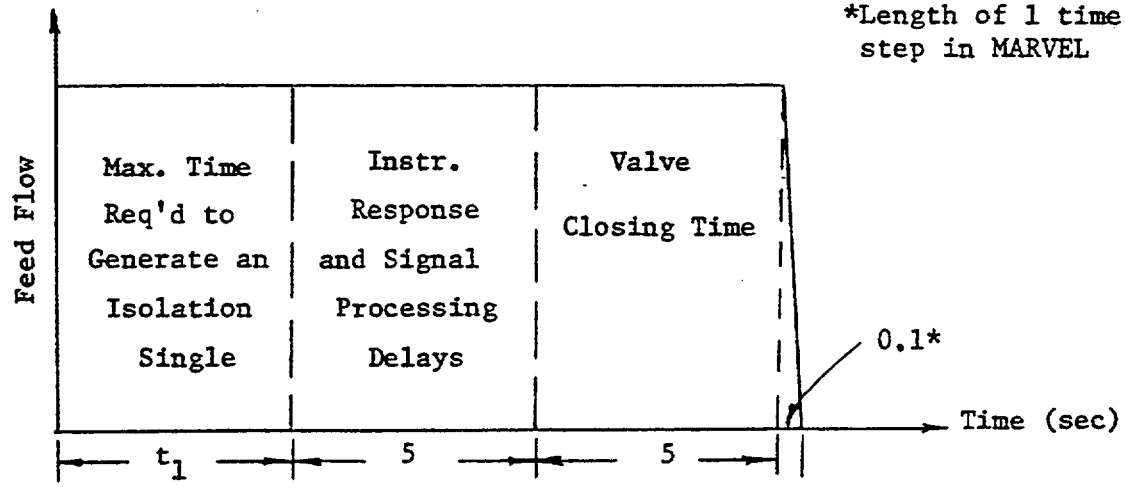
### QUESTION 2.11

Provide additional details of how the main feedwater flow to the ruptured steam generator is calculated before isolation. Discuss how the trip times given on page 4-20 and the five-second isolation time given on page 3-12 are used to calculate the feedwater isolation times given on page 3-16. Discuss how the feedwater isolation setpoints and isolation times in the tables of Part IV of Appendix A were determined. For each break provide the total amount of main feedwater assumed to flow to the ruptured steam generator. Discuss the methods by which applicants should calculate containment mass and energy release data in the event that feedwater flow exceeds the amounts assumed by the MARVEL code.

Answer 2.11

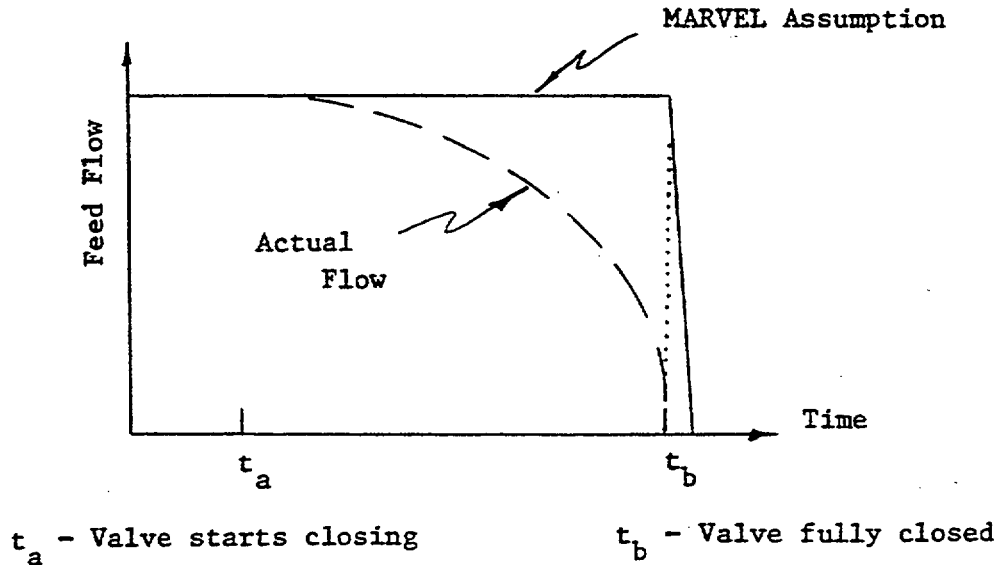
Feedwater flows used to determine the mass/energy releases presented in WCAP-8821 were not calculated. As discussed in Section 2.2.3, the TRANFLO studies to determine entrainment were performed assuming that the feed flow to the steam generator remained at its initial value for 10 seconds. This was done to minimize water entrainment since higher feed flows would have resulted in lower quality blowdowns in the TRANFLO calculations. However, since quality versus time data from TRANFLO was input directly to MARVEL, the MARVEL analyses assumed conservatively large feed flows to maximize the mass available in the steam generator for blowdown. The values of feed flow used in the MARVEL analyses are those quoted at the top of Page 3-16.

The time during which main feed is supplied to the steam generators in the MARVEL analyses for each of the doubled ended ruptures is also given on Page 3-16. The flow was held constant at the specified value for this entire time period. The series of factors which make up each of these times are defined in the sketch below.



The values chosen for each of the factors are conservative for several reasons. Functional design requirements for protection instrumentation and process equipment, for example, require that response and processing delays be much less than 5 seconds. as is conservatively used in these analyses. In general, these times on the order of 0.5 - 1.5

seconds depending upon which protection signal is considered. Also, though design requirements for isolation valves specify a maximum of 5 seconds for closure following a trip signal, closing times are often much shorter, and the flow versus time (during closing) follows a trend much like that shown below rather than the step change in flow used in the MARVEL analyses.



Further conservatism is included in  $t_1$ . The  $t_1$ 's used were determined with the MARVEL code by analyzing a large number of blowdowns from many break sizes and power levels to identify the set of input assumptions resulting in the longest delay prior to reaching a trip setpoint for isolation. These assumptions were then used to establish  $t_1$  for the breaks and power levels of interest. Conditions found to be important were the use of low feedwater flow rates prior to trip, correcting turbine steam flow for the steam pressure decay prior to turbine trip, assuming dry steam blowdowns, and using high values of initial steam generator mass. All of these assumptions tend to increase the rate of steam pressure decay following the break. Because this process was used, the values of  $t_1$  used to arrive at the times listed on Page 3-16 are generally significantly longer than the actual time that would be required to reach the isolation setpoint were more appropriate assumptions

made. (It should also be noted that the limiting values of time to reach the feedwater isolation setpoint quoted in the tables of Section IV, Appendix A, correspond to the times given on Page 3-16 minus 10.1 seconds).

In comparison, the "time to signal" values on Page 4-20 are the MARVEL calculated values of  $t_1$  for all sixteen breaks using the assumptions described in Section 3.0 of WCAP-8822, i.e. high feed flow, entrained moisture, etc. As can be seen, these times are consistently shorter than the values of  $t_1$  used in the determination of isolation times. Additionally, the times in Table 4-2 were used only to initiate a reactor trip sequence for the breaks at power and to initiate safety injection for the zero power cases. They were not used to initiate steam and feed isolation. Note also, as mentioned in the footnote on Page 4-20, the differences in the time between Table 4-2 and the times in Appendix A for the small DER's at zero power are due to a feed isolation signal being derived from a coincident reactor trip - low  $T_{avg}$  signal which occurs prior to the SI signal generated by low pressurizer pressure.

As a final comment on isolation times used in WCAP-8822, Table 4-2 was found to have three typographical errors. The split break entries for 70%, 30% and hot standby power conditions should be blank. The values shown are repeats of the entries for the preceding small DER. This should be corrected in your copies.

The probability of an applicant calculating higher feed flows than were assumed in the MARVEL analyses is very low. Current design requirements for Westinghouse plants require two valves in each feed line capable of closing within 5 seconds following an isolation signal, and typical system calculations of the maximum possible feed flow during a steam break event result in flow which are generally much lower than 300% of nominal flow during the early portion of a steam break depressurization transient. However, even if a particular plant design does result

in higher flows, the insensitivity of the blowdown releases to feed flow during the initial seconds (see Section 3.1.5) indicates that the data provided will still be applicable. The only requirement is to account for all of the water added to the steam generator by the feed system so that the effects on total energy release and steam generator dryout time are included in the containment analyses. Methods by which the accounting can be done are explained in Paragraphs III.1.A, III.1.D, III.2.A, and III.2.C of Appendix A of WCAP-8822.

## References

1. A. N. Nahavandi and R. F. VonHollen, "A Space-Dependent Dynamic Analysis of Boiling Water Reactor Systems," *Nuclear Science and Engineering*: 20, 392-413 (1964).
2. W. A. Massena, "Steam Water Pressure Drop and Critical Discharge Flow - A Digital Computer Program," General Electric, Hanford Atomic Products Operation, Richland, Washington, Report No. HW-65706, (1960).
3. R. E. Land and R. W. Steitler, "Modeling the Effect of Inventory Loss on Steam Generator Heat Transfer," AGME Technical Publication 76-WA/HT-70.
4. A. A. Armand, "The Flow Mechanism of a Two-Phase Mixture in a Vertical Tube," article in a book entitled Hydrodynamics and Heat Transfer with Boiling, ed. M. A. Styrikovich, Acad. Nauk SSSR, Moscow (1954).
5. H. S. Islain, et. al., "Void Fractions in Two-Phase Flow," *A.I. Ch. E Journal*, Vol. 5, No. 4 (1959).
6. S. Leoy, "Steam Slip-Theoretical Prediction from Momentum Model," *ASME Journal of Heat Transfer*, May 1960.
7. W. Idsinga, et. al., "An Assessment of Two-Phase Pressure Drop Correlations for Steam-Water Systems," *I.J.M.F.*, Vol. 3, No. 5.
8. "Satan VI Program: Comprehensive Space-Time Dependent Analysis of Loss-of-Coolant," WCAP-8302, June 1974.
9. S. Whitaker, Introduction to Fluid Mechanics, Prentice-Hall, Inc., 1968, pp. 300.

10. O. J. Mendler, et. al., "National Circulation Tests with Water at 800 to 2000 psia Under Nonboiling, Local Boiling, and Bulk Boiling Conditions," Journal of Heat Transfer, August 1961, pp 261-273.
11. S. G. Margolis, J. A. Redfield, "FLASH: A Program for Digital Simulation of the Loss of Coolant Accident," WAPD-TM-534, Westinghouse Electric Corp., May, 1966.
12. M. Y. Young, et. al., "Westinghouse Emergency Core Cooling System Evaluation Model Application to Plants Equipped with Upper Head Injection," WCAP-8479-P, Rev. 1 (1976)